Environmental Nanotechnology, Monitoring & Management 17 (2022) 100638

Contents lists available at ScienceDirect

Environmental Nanotechnology, Monitoring & Management

journal homepage: www.elsevier.com/locate/enmm

Pesticide elimination through adsorption by metal-organic framework and their modified forms

Valentino Bervia Lunardi [a], Felycia Edi Soetaredjo [a,*], Kuncoro Foe [b], Jindrayani Nyoo Putro [a], Shella Permatasari santoso [a], I. Gede Wenten [c,d], Wenny Irawaty [a], Maria Yuliana [a], Yi-Hsu Ju [e], Artik Elisa Angkawijaya [f], Suryadi Ismadji [a,*]

[a] Department of Chemical Engineering, Widya Mandala Surabaya Catholic University, Kalijudan 37, Surabaya 60114, Indonesia
[b] Biomedical Laboratory, Faculty of Pharmacy, Universitas Katolik Widya Mandala Surabaya, Jl. Kalisari Selatan No.1, Kalisari, Mulyorejo, Surabaya 60112, East Java, Indonesia
[c] Chemical Engineering Department, Institut Teknologi Bandung, Jalan Ganesa No. 10, Bandung 40132, Indonesia
[d] Research Center for Nanosciences and Nanotechnology, Institut Teknologi Bandung, Jalan Ganesa No. 10, Bandung 40132, Indonesia
[e] Graduate Institute of Applied Science and Technology, National Taiwan University of Science and Technology, Taipei 106-07, Taiwan
[f] Department of Chemical Engineering, National Taiwan University of Science and Technology, Taipei 106-07, Taiwan

ARTICLE INFO

Keywords:
MOF
Pesticides
Adsorption

ABSTRACT

For the healthy growth of living beings, accessibility to clean water is highly required. Tackling the removal of pesticides from aquatic systems should be a key research issue to restore ecosystem balance and ensure a more sustainable future. Due to its cost-effective and facile operation condition, adsorption is considered one of the most promising technologies for pesticide elimination. Currently, Metal-Organic Framework (MOFs) have sparked considerable scientific interest because of their fascinating structures and unique physical properties such as adjustable porosities, large pore volumes, hierarchical structures, and excellent adsorption and regeneration capabilities. Moreover, adding functional groups, magnetic moieties, and particular foreign substance incorporation would advance the MOFs' development and ameliorate their performance. Hence, this review critically summarized the ongoing development of MOF-based adsorbents for pesticide removal from an aqueous solution. Furthermore, Major interaction pathways between MOFs and pesticides are also proposed in response to various experimental circumstances, including pH, and coexisting ions, with an additional isotherm and kinetic study to clarify the adsorption mechanism. Eventually, several suggestions are made to develop MOFs with enhanced adsorption properties for pesticides removal.

1. Introduction

The development of various kinds of agricultural products accompanied by the emergence of pests and plant diseases encourages the excessive use of pesticides (Liu et al., 2019b). In 2016, 4.1 million tons of pesticides were consumed globally, with 51.3% percent utilized

Abbreviations: 2,4-D,A, Acid-Alkaline Interaction; ABI, Acid-base interaction; ACE, Acetomiprid; AOPs, Advance Oxidation Process; ALC, Alachlor; ATR, Atrazine; BA, Boric acid; C, Coordination or Covalent Bond; CAUs, Christian-Albrecht's-University series; CCDC, Cambridge Crystallographic Data Centre; CFA, Clofibric Acid; CTAB, Cetyltrimethylammonium bromide; CTN, Chlorantraniliprole; CTP, Chipton; CTN, Clothianidin; D, Diffusion Controlled; DA, Dubinin-Asthakov; DEET, N,N-Diethyl Meta Toluamide; DHV, Dichlorvos; DMT, Dimethoate; DUR, Diuron; DTF, Dinotefuran; DZ, Diazinon; e^-, Electrostatic Interaction; ETH, Ethion; ETP, Ethoprop; F, Freundlich; GO, Graphene Oxide; GF, Glufosinate; GMX, Gramoxone; GP, Glyphosate; H, Henry; h, Hydrophobic Interaction; H, Hydrogen Bond Interaction; IDP, Imidacloprid; IE, Ionic Exchange; IL, Ionic Liquid; IZF, Isazofos; L, Langmuir; MCPP, Methylchlorophenoxypropionic acid; MOFs, Metal-organic frameworks; MILs, Materiaux de l'Institut Lavoisier; MPRT, Methyl-Parathion; MTD, Methidathion; MTF, Metrifonate; MWCNTs, Magnetic Walled Carbon Nanotubes; NB, Nitrobenzene; NPC, Nanoporous carbon; NTR, Nitenpyram; PCNs, Porous Coordination Network Series; PF, Pore-filling; PFO, Pseudo First Order; PFOS, Perfluorooctanesulfonate; PNP, P-Nitrophenol; PSO, Pseudo Second Order; PSN, Phosalone; PNF, Profenofos; PTH, Prothiofons; R-P, Redlich Peterson; S, Sips; SBUs, Secondary building units; SFP, Sulfotep; T, Temkin; TCP, Thiacloprid; TDF, Triadimefon; TMX, Trimethoxam; Ttb, Tebuthiuron; TZP, Triazophos; UIO, Universetet I Oslo; ZIFs, Zeolitic Imidazolate Frameworks.

* Corresponding authors.
E-mail addresses: felyciae@yahoo.com (F. Edi Soetaredjo), suryadiismadji@yahoo.com (S. Ismadji).

https://doi.org/10.1016/j.enmm.2021.100638
Received 29 October 2021; Received in revised form 19 December 2021; Accepted 27 December 2021
Available online 3 January 2022

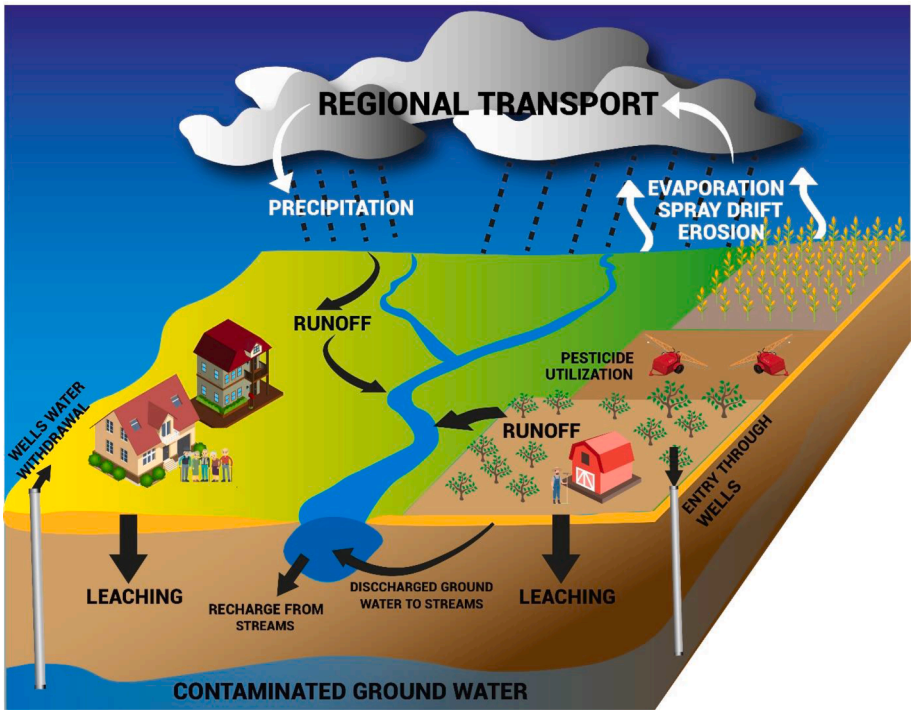

Fig. 1. Pesticides transfer routes to surface and ground water.

in Asia, 33.3% in the Americas, 11.8% in Europe, 2.2% in Africa, and 1.4% in Oceania. In vast quantities, pesticides used in agriculture consist of fungicides, herbicides, and insecticides (29%, 46%, and 17% of a total of 4.1 million tons, respectively) (Mojiri et al., 2020). Nevertheless, only 1% of pesticides successfully exerted to the specified targets while the rest of 99% were drawn off toward soil and waterbody via diffusion through surface runoff, erosion, spray-drift, and leaching (Ali et al., 2019; Cosgrove et al., 2019) (Fig. 1). These substances have been classified as persistent organic pollutants and may expose severe damage to the ecological system and human health, including irritation, nervous and endocrine system damage, and carcinogenic effects (Kim et al., 2017; Sabarwal et al., 2018). It is crucial to develop advanced water treatment technology to effectively remove the pesticides from water to conserve environmental safety and public health protection.

Scientists have explored a promising way of pesticide elimination through physical (membrane filtration), chemical (chlorination, Advanced oxidation process (AOPs) ozonation), and biological treatment (aerobic and anaerobic treatment, activated sludge, and membrane bioreactor). Each method provides its benefits and drawbacks in terms of technical (e.g., efficiency, operability, reliability, environmental aspect, pre-treatment requirement, toxic byproducts, and sludge production) and economic aspect (e.g., capital and operational cost). For detailed methodology, the discussion has been well-presented elsewhere (Saleh et al., 2020). Adsorption has been pointed out as promising technology for pollutants removal with comparative benefits, including a low-cost, non-complex system, no harmful secondary pollutants, and facile adsorption and regeneration operation (Al-Ghouti and Da'ana, 2020).

The adsorbent is the crucial factor of pesticide adsorption since the adsorption efficiency is mainly evaluated based on the adsorbents' capacity, selectivity, kinetic, and regeneration. Regarding adsorbent characteristics, the porosity and geometry, along with specific adsorption sites, contribute significantly to the efficiency of organic pollutants removal (Wang and Guo, 2020). In addition, the incorporation of diverse functional groups or active sites towards porous materials can refine the selectivity and capacity for pesticide loading (Joseph et al., 2019). Therefore, further exploration is required to find and construct new

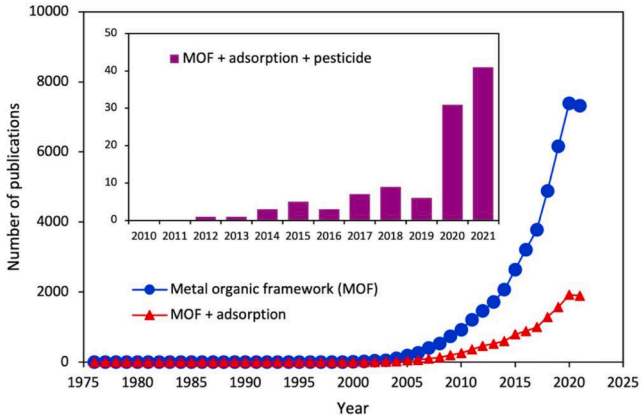

Fig. 2. The number of publications related to the metal–organic framework (MOF), MOF for adsorption applications, and pesticide adsorption using MOF indexed by Scopus. Queries: TITLE-ABS-KEY (terms), accessed on October 23rd, 2021.

functional adsorbents since most common adsorbents like zeolite, clays, and activated carbon exhibit finite porosity and functionalities, which are un-flexible for various modifications (Li et al., 2018). Hence, the advancement of novel adsorbents with better performance is necessary for pollutants remediation. In the current years, Metal-Organic Framework (MOFs) have registered to overcome the handicap of the past adsorption system as indicated by the increasing number of papers published (Fig. 2). This review inaugurated the MOFs overview and subsequently provided several strategies for improving pesticide removal efficiency through adsorption.

2. Overview of MOFs

2.1. Brief discussion on MOFs and their synthesis

Well-built coordination bonding between metal cations salts or

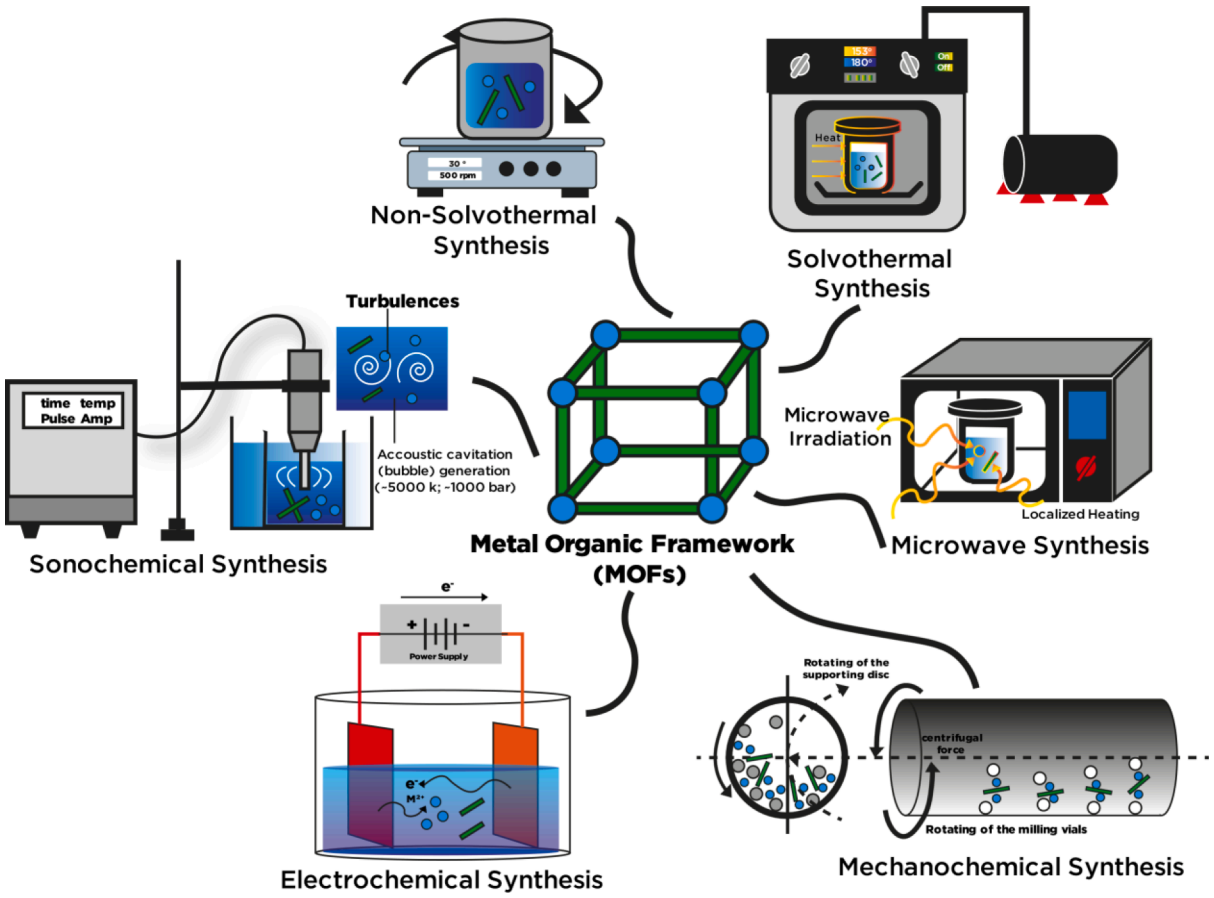

Fig. 3. Different methods of MOF synthesis.

clusters and polydentate organic ligands construct secondary building units (SBUs) can create 1D (chains), 2-D (layers), and 3-D (Framework) open porous crystalline materials with infinite lattices. These types of coordination are classified into porous inorganic–organic hybrid or known as Metal-Organic Framework (MOFs) (Safaei et al., 2019). The coordination preferences of SBUs crucially determine the MOFs formation along with the length and stiffness of organic linkers at the mercy of variegated reaction environments such as solvent types, temperature and time reaction, and the ratio of metal ion to ligands (Guan et al., 2018). A typical approach of MOF preparation is a bottom-up strategy in which the straight-forward reaction occurs between metal and organic ligands under established reaction conditions to assure the oriented crystal growth. Several factors such as the physicochemical characteristic, economic, and environmental aspects should be considered for the suitable MOFs synthesis and future scale-up possibilities.

Conventional methods include solvothermal, and non-solvothermal synthesis is the most common process to synthesize MOFs since they provide facile operation. In the solvothermal synthesis, the crystallization occurs in a sealed vessel comprising of solvent with the metal ions, organic ligands, and other composite material where the high temperature and pressure (above solvent boiling points) are required to assist the self-assembly and crystal formation. The solvent selection is vital, which impacts the reactant solubility and reaction temperature. Hydrothermal synthesis employed water as dispersive media instead of an organic solvent, which is cheaper, safer, and more straightforward. In this method, the crystallization energy is provided by conventional electric heating within several hours and up to days to initiate and stimulate the synthesis reaction. Meanwhile, the non-solvothermal synthesis utilizes less equipment and can be accomplished in an open vessel.

Currently, the microwave technique induces MOFs formation by adding electromagnetic waves at 300 MHz to 300 GHz frequency, providing a shorter time reaction even in a minute's reaction without any defiance in crystal quality. The utilized frequency generates heat by inducing the collision of rotating polar solvent molecules and facilitating the interaction between microwaves and electric charges of irradiated molecules. On the other hand, the sonochemical synthesis uses ultrasonic waves at a frequency range from 20 kHz to 10 MHz, initiating the cavitation effect, which depends on the bubble formation, followed by their growth and disintegration. This technique intensified high local pressure (up to 1000 bar) and temperature (up to 5000 k) and catalyzed the chemical reactions. The electrochemical technique has favorably constructed MOF layer thin film when the electric current circulated via electrochemical cell comprising of metal cathode immerse in electrolytes solution consists of organic linkers. Instead of using metal salts, the metal sources are simultaneously supplied through anodic dissolution, promoting the coordination of metal ions and deprotonated ligands in the electrolyte solution (Li et al., 2016b). The previous studies required a solvent to enhance the mobility of metal ions and organic ligands, which assist the chemical reaction and the coordination bonds formation. In the meantime, a typical mechanochemical reaction occurs through mechanical energy absorption by reagents (commonly in the solid form) throughout the milling/grinding process under a solvent-free environment. Adequate energy is released by friction and impact between balls and reactants, which provoke a chemical reaction. High energy grinding/milling system is required to cause structural stress, coordination breakage, and reactive radical formation, which exposed the atom's reactive layers and subsequently expedited the chemical reaction on the solid reactants interface. Fig. 3 schematically presents the type of MOFs synthesis. A more detailed discussion of MOFs synthesis was provided elsewhere (Stock and Biswas, 2012).

Until now, Cambridge Crystallographic Data Centre (CCDC) has

Table 1
The current progress of pesticides removal through adsorption by MOF and its modification.

Materials			Target	Operation Parameters				Adsorption Modelling				Ref.
Types	Surface area (m^2/g)	Pore size (nm)		Adsorbent dosage (g/L)	t (h)	T (K)	pH	Kinetic[b]	Isotherm[c]	Q_{max} (mg/g)	Mechanism[d]	
Virgin MOFs												
MIL-53 (Cr)	1438	micropore	2,4-D	0.1	12	298	2.8	PSO	L	556	e^-; π–π; P	(Jung et al., 2013)
MIL-53 (Al)	866	n.d.	DMT	0.04 g	8	303	–	PSO	L	154.8	e^-; P	(Abdelhameed et al., 2021b)
	1235	n.d.	NB	0.1	0.5	303	7.2	PSO	S; R-P	610	π–π; h	(Patil et al., 2011)
MIL-68 (Al)	1417	0.6–0.64;1.6–1.7	NB	0.1	2	303	6	PSO	L	1188.3	e^-; H	(Xie et al., 2014)
MIL-100 (Fe)	1893	2.2	2,4-D	0.5	6	303	3	PSO	S	858.11	ABI; PF; e^-	(Tan and Foo, 2021)
MIL-101 (Cr)	2611.79	1.9	DZ	0.5	1.08	298	6.5	–	L	19.58	C; π-CM;	(Mirsoleimani-azizi et al., 2018)
	3900	–	MCPP	0.1	12	298	4	–	–	~<10	–	(Seo et al., 2015)
ZIF-8 (Zn)	n.d.	n.d.	ETH	1	8	303	7	PSO	L	366.7	H; π–π; C	(Abdelhameed et al., 2019)
			PTH					PSO	L	279.3		
	1875	micropores	ATR	0.6	0.033	298	–	PSO	S	9.95	h; π–π	(Akpinar and Yazaydin, 2018)
	1758	1.76	BA	5	12	313	4.42	PSO; IPD	F; H	247.44	C	(Lyu et al., 2017)
ZIF-67 (Co)	n.d.	n.d.	ETH	1	8	303	7	PSO	L	261.1	H; π–π; C	(Abdelhameed et al., 2019)
			PTH					PSO	L	210.8		
	1776	1.2–3	BA	3	5	298	4	PSO	H	579.80	e^-; π–π; C	(Zhang et al., 2019a)
UIO-66 (Zr)	1423	n.d.	PFOS	0.5	1	298	5	PSO; PFO;	L; F	620.16	ABI; PF; e^-; IE; h	(Clark et al., 2019)
	1500	n.d.	DHV	0.8	3.5	298	4	PSO	L	172.40	C; D	(Jamali et al., 2019)
		n.d.	MTF							90.49	D	
	982	n.d.	MCPP	0.1	24	298	3.8	PSO	L	370	e^-; π–π	(Seo et al., 2015)
UIO-67 (Zr)	2400	n.d.	DHV	0.8	3.5	298	4	PSO	L	571.43	C; D	(Jamali et al., 2019)
		n.d.	MTF							251.19	D	
	2172	1.17;1.61;2.3	GP	0.03	5	298	4	PSO	L	537	C; D	(Zhu et al., 2015)
			GF				5			360		
	2345	micro-mesopores	ATR	0.6	0.67	298	–	PSO	F	~29 mg/g	h; π–π	(Akpinar and Yazaydin, 2018)
	n.d.	n.d.	GP	0.06	6	298	n.d.	PSO	L	1335	ABI	(Pankajakshan et al., 2018)
NU-1000 (Zr)	n.d.	n.d.	GP	0.06	6	298	n.d.	PSO	L	1516	ABI	Pankajakshan et al., 2018)
	2210	1.2;3	ATR	0.35	2	RT	n.d.	–	L	36	π–π	(Akpinar et al., 2019)
Calcium Fumarate MOFs	2308.03	15.23	IDP	1	5	298	7	PFO	L	467.23	C	(Singh et al., 2021)
Al-TCPP (nanosheet form)	1359	Macro/Meso/ Microporous	CTP	0.5	3	298		PSO	F	371.91	PF; HP	(Xiao et al., 2021)
Al-TCPP (bulk crystal)	1296	Microporous								222.11		
Functionalized MOF												
NH_2-MIL-53 (Al)	1060	n.d.	DMT	0.04 g	8	303	–	PSO	L	266.9	e^-; H	(Abdelhameed et al., 2021b)
Al-$(BDC)_{0.5}(BDC\text{-}NH_2)_{0.50}$	1260	n.d.	DMT	0.04 g	8	303	–	PSO	L	513.4	e^-; H	(Abdelhameed et al., 2021b)
NH_2-UIO-66 (Zr)	604.19	n.d.	2,4-D	1	12	298	3	PSO	L	72.99	e^-; H; π–π	(Li et al., 2020a)
UIO-66-NMe_3^+	484	0.51; >=0.88	2,4-D	0.1	2	298	2	PSO	L	279	e^-; π–π, π-MC; ABI; IE	(Wu et al., 2020)
CAU-1	1281	0.45;1	NB	0.1	2	303	6	PSO	L	1171.65	e^-;H	(Xie et al., 2014)
ED-MIL-101	2555	n.d.	CFA	0.1	2	298	n.d.	PSO	L	347	ABI; π–π	(Hasan et al., 2013)
AMSA-MIL-101	2322									105		
NH_2-MIL-101 (Cr)	1597	1.9	GP	2	12	298	3.7	PSO; IPD	F	64	e^-	(Feng and Xia, 2018)
UR_2-MIL-101 (Cr)	1253	0.6							L;F	25		
MIL-101 (Cr) (C_1)- Furan	951.3	n.d.	DUR	0.75	6	298	7	n.d.	n.d.	148.97	H; π–π	(Yang et al., 2019)
			ALC							122.72		
			TTh							79.47		
			GMX							49.05		
MIL-101 (Cr) (C_1)-2-Methyl Furan	502.6	n.d.	DUR	0.75	6	298	7	n.d.	n.d.	135.87	H; π–π	
			ALC							107.67		
			TTh							73.35		
			GMX							45.41		
MIL-101 (Cr) (C_3) – 2-ethyl furan	490.6	n.d.	DUR	0.75	6	298	7	n.d.	n.d.	141.42	H; π–π	
			ALC							104.02		
			TTh							69.71		
			GMX							50.18		
MIL-101 (Cr) (C_4) – (Thiophene)	492.4	n.d.	DUR	0.75	6	298	7	n.d.	n.d.	161.25	H; π–π	

(*continued on next page*)

Table 1 (*continued*)

Materials			Target	Operation Parameters				Adsorption Modelling				Ref.
Types	**Surface area (m^2/g)**	**Pore size (nm)**		**Adsorbent dosage (g/L)**	**t (h)**	**T (K)**	**pH**	**Kinetic[b]**	**Isotherm[c]**	**Q_{max} (mg/g)**	**Mechanism[d]**	
			ALC							105.15		
			TTh							81.73		
			GMX							64.11		
MIL-101 (Cr) (C_5) (bromide furan)	543.2	n.d.	DUR	0.75	6	298	7	n.d.	n.d.	186	H; π–π	
			ALC							149.79		
			TTh							94.57		
			GMX							57.99		
MOF based Composites												
ZIF-8@MCPA	6.416	90.28	CPT	0.125	35	303	7	PSO	L	160.9	H; π–π	(Liang et al., 2021)
			ALC				5			199.47		
UIO66-NH_2 @MCPA	8.872	78.37	CPT				4			246.8		
			ALC				5			247.52		
UIO-67/GO	GP	n.d.	n.d.	0.02	3	RT	4	PSO	L	482.69	e^-; C; H	(Yang et al., 2017)
Fe_3O_4@SiO_2@UIO-67	n.d.	n.d.	GP	0.03	2	RT	n.d.	PSO	L	256.54	C	(Yang et al., 2018)
M−MOF	250.33	n.d.	TMX	5	1	n.d	n.d.	PSO	F	n.d.	H; h; e^-; π–π	(Liu et al., 2017)
			IDP									
			AMP									
			NTR									
			CTN									
			TCP						L			
M−M−ZIF−8	127.95	n.d.	TZP	3.75	0.83	RT.	4	n.d.	F	3.12	C	(Liu et al., 2018)
			DZ							2.59		
			PSN							3.80		
			PNF							3.89		
			MTD							2.34		
			ETP							2.18		
			SFP							2.84		
			IZF							3.00		
M−ZIF−8@ZIF-67	219	n.d.	FP	3.75	0.75	RT	6	PSO	F	–	e^-; ABI; π–π	(Li et al., 2020b)
Cu-BTC@Cotton	n.d.	n.d.	ETH	1.125	2	n.d.	n.d.	PSO	L	182	PF; C	(Abdelhameed et al., 2016)
Cu-BTC@CA	965.8	n.d.	DMT	0.8	6	313	7	PSO	L	321.9	e^-, H, C	(Abdelhameed et al., 2021a)
ILCS/U-10	198.37	30.47	2,4-D	0.1	1	298	2.97	PSO	T	246	e^-, H; π–π	(Huang et al., 2020)
BSA/PCN-222 (Fe)	1015	1.09;2.73	MPRT	0.12	0.05	AT	7	n.d.	L	370.4	e^-; H; h; π–π; PF	(Namdar Sheikhi et al., 2021)
			DZ					n.d.		400	e^-; H; h; π–π; PF; ABI	
Fe_3O_4@ZnAl-LDH@MIL-53(Al)	726.1	5.2	TDF	30	0.083	308.15	6	PSO	L	46.08	H, C; π–π	(Lu et al., 2021)
			EXZ					PFO; PSO		71.79		
MOF derived Materials												
CeO_2	n.d.	n.d.	2,4-D	0.25	2	308	n.d.	PSO	L; F; S	95.78	e^-; π–π	(Abdelillah Ali Elhussein et al., 2018)
β-CD MOF-NPC	263.7	Micropore	MET	10 mg	2	n.d.	n.d.	PSO	L	343.42	e^-; H; π–π	(Liu et al., 2019a)
			ALC							291.26		
			ACE							261.21		
			PRE							311.78		
IMDC	1421	Mesopores	ATR	1	12	298	n.d.	PSO	L	208	H	(Ahmed et al., 2017)
IMDC	1468	n.d.	2,4-D	0.1	12	RT	3.5	PSO	L	448	H; h; π–π	(Sarker et al., 2017)
			DUR				6.6			284		
ZnO/$ZnFe_2O_4$	104	9.14	ATR	0.4	72	298	7	n.d.	DA	n.d.	H; h	(Chen et al., 2017)
CDM-74	1395	n.d.	DEET	0.12	12	n.d.	7	n.d.	L	340	H	(Bhadra et al., 2020)

a Targeted Pesticides: 2,4-D: 2,4-Dichlorophenoxyacetic acid; DMT: Dimethoate; ETH: Ethion; PTH: Prothiofons; PNP: P-Nitrophenol; DZ: Diazinon; PFOS: Perfluorooctanesulfonate; DHV: Dichlorvos; MTF: Metrifonate; GP: glyphosate; GF: glufosinate; ATR: Atrazine; MCPP: Methylchlorophenoxypropionic acid; IDP: imidacloprid; NB: Nitrobenzene; BA: Boric acid; DUR: Diuron; ALC: Alachlor; Tth: Tebuthiuron; GMX: Gramoxone; TMX: Trimethoxam; ACE: Acetamiprid; NTR: Nitenpyram; DTF: Dinotefuran; CTN: Clothianidin; TCP: Thiacloprid; TZP: Triazophos; PSN: Phosalone; PNF: Profenofos; MTD: Methidathion; ETP: Ethoprop; SFP: Sulfotep; IZF: Isazofos; CFA: Clofibric acid; MPRT: Methyl-Parathion; TDF: triadimefon; CTN: chlorantraniliprole; CTP: Chipton; DEET: N,N-Diethyl Meta Toluamide.

[b] Kinetic equation: PSO: Pseudo Second Order; PFO: Pseudo First Order.

[c] Isotherm equation: L: Langmuir; F: Freundlich; S: Sips; T: Temkin; R-P: Redlich Peterson; H: Henry; DA: Dubinin-Astakhov.

[d] Mechanisms: electrostatic interaction (e^-), hydrophobic interaction (h), π-π interaction (π-π), π-complex formation with cations (including metal or positive ion charge groups) (π-CM), Hydrogen bond interaction (H), acid-alkaline interaction (A), coordination or covalent bond (C), pore filling (P); Ionic exchange (I); Ion exchange (IE); Diffusion controlled (D).

recorded over 15,000 MOFs with a diverse selection of metal clusters or organic linkers (Coudert and Fuchs, 2016). Such a wide selection of metal ions including Fe(III), Cu(II), Ca(II), Al(III), Mg(II), Zn(II), Cd(II), Co(II), Zr(IV), Ln(III), and Ti(III) and organic ligands containing cyano and pyridyl, carboxylates, phosphonates, and crown ethers were capable of constructing different porous geometries such as trigonal bipyramidal, pyramidal, square, tetrahedral and octahedral (Long and Yaghi, 2009). Owing to the MOFs structure flexibility, it can be modulated based on the porosity metrics, functionalities, architectures, and shape from microporous to macroporous scale for the specific field of applications, including catalyst (Lee et al., 2009), energy storage (Baumann et al., 2019), biomedical (Keskin and Kızılel, 2011), sensing (Lei et al., 2014) and environmental remediation (Kumar et al., 2020). Specific modification is required to enhance guest molecules' selectivity and uptake efficiency.

It is worth mentioning strategy to architecture hierarchical porous MOFs comprising mesoporous/macroporous structure. Even though MOFs structure is versatile and variable, several MOFs have microporous structures (pore size < 2 nm), limiting the bulky molecules diffusion and its interaction with the active site within the MOFs framework. Guan et al. (2018) highlighted several types of synthesis, including template (surfactant-assisted synthesis) or template-free synthesis, gelation strategy, modulator induce defect formation, metal–ligand fragment co-assembly, and supercritical fluid have performed for mesoporous or macroporous creation (Guan et al., 2018). The existence of meso/macro structured to provide significant enhancement in the diffusivity and mass transfer for large molecules adsorption and separation, drug delivery, and heterogenous catalyst. Moreover, meso/macropores in the fabricated microporous MOFs refine the accessibility of active sites inside the microporous structures. In addition, this strategy also facilitated host or anchoring of various active sites precursor which ease the MOFs modification without any diffusion restriction in confined space which open-up new possibilities for various implementation with novel characteristics.

2.2. Current strategies of MOFs as adsorbent

In recent years, the MOFs utilization in water treatments has been sought after in adsorption and AOPs. Among diverse environmental remediation strategies, removing pollutants such as dye (Uddin et al., 2021), metal ions (Li et al., 2018), and pharmaceutical and personal care products (Jin et al., 2020) by adsorption have been well-reviewed. Nonetheless, the detailed strategy of pesticide and its derivative removal through MOFs still limited Scientist mainly exploited only a few types of MOFs such as ZIFs (ZIF stand for Zeolitic Imidazolate Framework), MILs (Material Institute Lavoisier), PCN (Porous coordination network), UIOs (University of Oslo) and NU (Northwestern University) since they effectively eliminate organic pollutants. Table 1 presents current MOFs used for pesticides adsorbent and their current chemical configurations. The MOFs adsorption ability has been evaluated based on the adsorption isotherm, kinetics, thermodynamics, selectivity, and recyclability. These features are regulated by physicochemical characteristics, hydrophilicity, functionality, and well-organized framework structures. Commonly, the higher surface area adsorbent impacts the adsorption performance (Lei et al., 2017).

Nevertheless, the common phenomena will occur when Van Der Waals collision is the primary adsorption mechanism (Sarker et al., 2018). In several cases, the adsorbate affinity towards MOFs has a remarkable impact as well. The affinity of organic pollutants onto MOFs follows through several primary mechanisms such as the electrostatic interaction, hydrophobic, acid-base interaction, hydrogen bonding, and π-complexation. Specific MOFs also present pore size and shape selectivity adsorption for organics contaminants in water.

A strategy of refining the performance of MOFs adsorption has captivated scientists in the past few years. Several MOFs categories have been well developed: (1) **MOFs constructed based on longer organic linkers (ligand extension technique)**. The MOFs porosity (e.g., MIL-101 (Cr), NU-1000, UIO-67, UIO-68) can expand up to 9.8 nm for MOFs by elongating the ligand length to 5 nm. This method is promising for improving the diffusion rate of organic pollutants towards MOFs. Nevertheless, the defect of structural interpretation of constructed MOFs with the ligand extension method is often observed, reducing the pore size significantly (Guan et al., 2018). (2). **The MOF-based on defect strategy**. A structural defect on MOFs structure often increases pore size and refines the accessibility and availability of active sites. Particularly, this method required modulator in the reactants mixture to create the defects (Fang et al., 2015); (3) **MOF-based on organic linkers functionalization**. Functional groups are incorporated into MOFs via traditional synthesis conditions utilizing organic linkers identical to pristine ligand but with attached functional groups (e.g., NH_2, $–NO_2$, –OH, -SH). The presence of specific functional groups can enhance the number of active adsorption sites and the parent MOFs' selectivity. (4) **MOF-based metal nodes functionalization**. Specific molecules can modify the metal cluster in the MOFs framework. Because of steric hindrance, functional groups bound to the metal cluster are often more active than those integrated into organic ligands. A common method such as post-synthetic ligand exchange and post-synthetic modification has been utilized to incorporate functional groups onto MOFs (Yin et al., 2019). (5) **MOF-based composite.** MOFs have been integrated with other functional materials such as magnetic MOFs (Fe_3O_4) and Graphene Oxide (GO) to enhance their adsorption capability. The magnetic MOFs are beneficial for recovery and regeneration adsorbent, which is a crucial factor in the practicability of MOFs. Meanwhile, the integrated MOFs with other adsorptive materials like graphene oxide have provided characteristic synergistic improvement with additional functional groups, porosity, and active sites compared to individual counterparts. Two strategies of MOFs composites production, including bottles around the ship and the ship in a bottle, have been widely used (Zhu and Xu, 2014). (6) **MOF-derived porous carbon materials**. Highly porous (nano or mesoporous) carbon materials can be procured by pyrolyzing MOFs at high temperatures under a protective atmosphere. Most MOFs derived porous carbon acquired integrated metal and carbon materials elements with multi-porous structure, which improves the diffusivity and mass transport of organic pollutants towards adsorbent. The existence of metal acting as active adsorbent sites with abundant functional groups from carbon materials will provide multiple possibilities for the adsorption of organic pollutants. In common, direct pyrolysis has been extensively used for MOFs-derived porous carbon materials (Yu et al., 2021). The current strategy of improving MOFs performances in adsorption has been schematically presented (Fig. 4).

2.3. Current study on MOFs stability and improvement

Undoubtedly, the MOFs have contributed to the refinement of practical application sustainability. Unfortunately, the reliability of MOFs in any form of application is not accompanied by chemical, mechanical, thermal, and water endurance. The frail aspect of the framework of MOFs is the metal–ligand coordination linkage which is prone to decomposition or degradation (Wang et al., 2016). In common, thermal and mechanical stability refers to the MOFs' ability to preserve their structural integrity under exposure to heat, pressure, or vacuum treatment environment. Meanwhile, the chemical stability is mainly related to the MOFs durability to the effect of different chemical environment exposure such as moisture, solvent, acidic, basic or anions or cations contained solutions. The thermal stability also corresponds with chemical stability because the chemical structure of MOFs can be altered through chemical reaction acceleration or initiation, which provokes crystalline framework degradation. The organic linker can suffer from decarboxylation or alkene oxidation, while the metal cations can undergo hydroxyl or redox activity, affecting the coordination bonding or organic ligand and inorganic ligand in MOFs structures (Mouchaham et al., 2018). The affinity of water towards MOFs exhibit competing

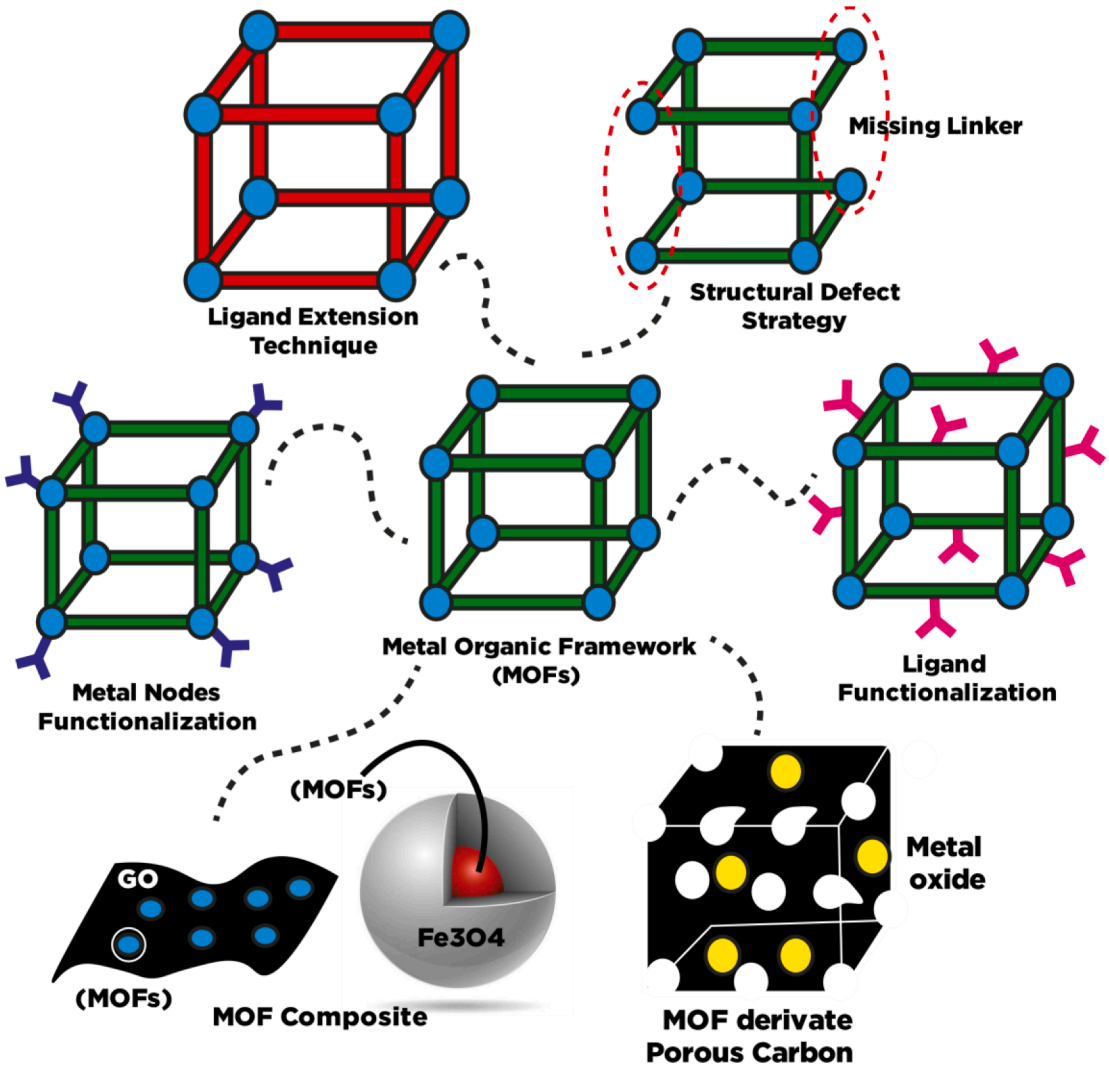

Fig. 4. Current strategy of improving adsorption performances of MOFs.

coordination between water molecules and organic linkers towards metal cluster/ metal ions. The water molecules have the probability of substituting the existing coordination, which further can destroy the framework if the metal–ligand coordination is weak enough (Burtch et al., 2014). Most MOFs exhibit a lack of durability to the above practical environment, which becomes the primary limitation on the continuity of MOFs' practical applications.

Theoretically, the MOFs' stability relies on the thermodynamic and kinetic aspects under the operational environment (Howarth et al., 2016; Yuan et al., 2018). The thermodynamics aspect refers to the strength of metal–ligand coordination. Evaluating the coordination strength in MOFs framework can be used for preliminary prediction on MOFs stability. The metal–ligand bond strength with specific ligands is positively associated with the metal cation charge and negatively linked with the ionic radius. In these terms, the charge and radius impact correlate to the charge density theory. Higher valent metal ions with high charge density provide a more stable framework for the same ligand and coordination environment, owing to stronger coordination bonds in line with Pearson's hard-soft -acid-base (HSAB) principle. Briefly, the lower valent metal ions generate a robust framework with relative higher pKa ligands (e.g., azoles), while the higher metal ions tend to provide a stable structure with relative lower pKa ligand (carboxylic acid).

Based on the HSAB theory, a more stable framework could be generated by coordinating hard acid-hard base and soft acid-bases (Devic and Serre, 2014). Hard acidic metals such as Cr3+, Al3+, Fe3+, and Zr4 + have successfully formed a robust coordination framework with carboxylate-based ligand as hard bases. In early-stage development, common MOFs based carboxylate ligand such as the MILs group (MIL-53 (Fe), MIL-101, MIL-101) (Férey et al., 2003; Férey et al., 2005) and UIO (UIO-66, UIO-67, and UIO-68) (Kandiah et al., 2010; Øien-Ødegaard et al., 2016; Yang et al., 2014) present remarkable stability. As time progresses, researchers have reported several MOFs such as the Christian-Albrecht's-University series (CAU-1, CAU-10, and CAU-17) (Hinterholzinger et al., 2010) and porous coordination network series (PCN-66, PCN-250, and PCN-222) (Feng et al., 2012; Ma et al., 2008) with remarkable stability. Recently, soft divalent metal ions (e.g., Zn^{2+}, Cu^{2+}, Ni^{2+}, Mn^{2+}, Ag^{2+}) construct highly stable MOFs with soft base azolate ligands (e.g., imidazolates, pyrazolates, triazolates, and tetrazolates). Zeolitic imidazolate frameworks present the most popular instances for this MOFs coordination (ZIFs) assembled with Zn^{2+} and imidazolate ligand (Chen et al., 2014). Meantime, other transition metal ions (e.g., Ni^{2+}, Cu^{2+}, Co^{2+}) successfully synthesized water-stable MOFs with strong basic resistance with triazolate and pyrazolate ligand (Bosch et al., 2017).

In terms of kinetic aspect, the stiffness of linker, framework interpenetration, number of coordination, and surface hydrophobicity influence the MOFs stability (Ding et al., 2019; Howarth et al., 2016; Yuan et al., 2018). In common, the higher stability has been demonstrated by rigid framework on account of outstanding durability towards lattice

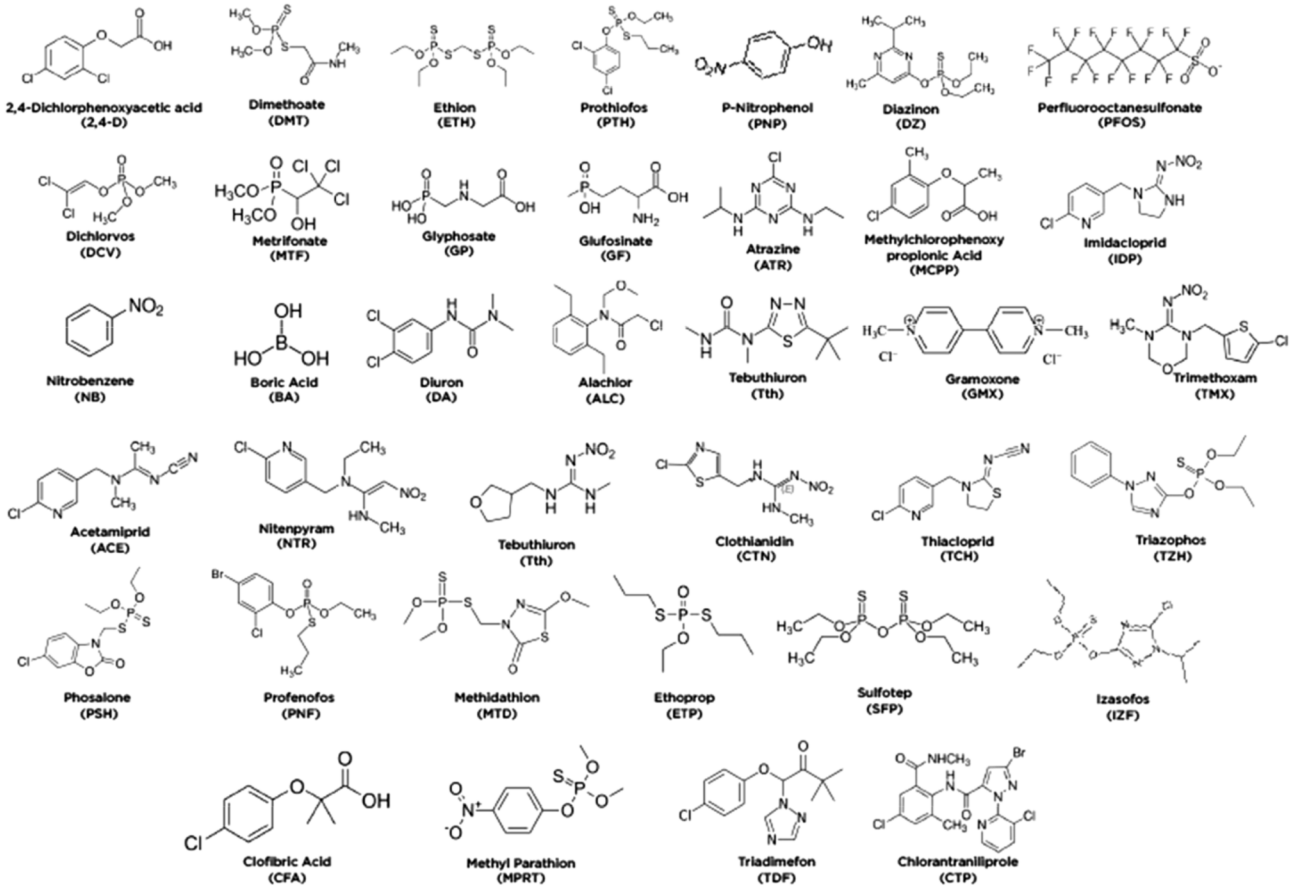

Fig. 5. Pesticides structure.

disintegration (Lv et al., 2019; Yuan et al., 2018). This presents the main stability pointed out to metal–ligand interaction but the not the only parameter to improve the stability. The porosity and geometrical structure and the vulnerability of the active site are also underlined as other key parameters. When the metal nodes and framework configuration remain the same, the linker and pore size enlargement deteriorate the MOFs' chemical stability (Ding et al., 2019) (for instance, UIO-66 (Cavka et al., 2008) and SUMOF-7 (Yao et al., 2015)). The active sites vulnerability can be ameliorated through incorporating hydrophobic moieties such as alkyl and fluorinated groups (Taylor et al., 2012; Yang et al., 2007; Yang et al., 2011), metal doping (Li et al., 2012), integration with other materials (e.g., graphene oxide (Zu et al., 2014), surface coating with polydimethylsiloxane (Zhang et al., 2014)) and MOF-derivate porous materials (e.g. (porous carbon (Sun et al., 2019), metal oxides (Xie et al., 2019)). These modifications possibly construct a shield by fun immobilizing functional groups either on the surface or decorating the internal structure, which effectively prevents the probability of ligand displacement by water molecules or enhances the water or moisture stability by inducing hydrophobic characteristics on the porous structure. These modifications prevent the possibility of water molecules' penetration or water molecules condensation towards crystal lattice and thus stave off framework destruction. In another strategy, the increasing steric hindrance for ligand displacement and systematic energy reduction on the interpenetrated framework improved the MOFs' stability (Burtch et al., 2014; Jiang et al., 2013).

Indeed, chemical stability is evinced as a prominent aspect to meet the implementation of MOFs for numerous applications (Ding et al., 2019; Howarth et al., 2016; Yuan et al., 2018). This is mainly for application in an aqueous environment with/without a difference, including organic molecules separation or drug transportation (Horcajada et al., 2010). Meanwhile, thermal and chemical stability is also critical for catalytic processes in a harsh environment to generate chemical feedstock and fuel (Vogt and Weckhuysen, 2015). Mechanical stability is primarily reckoned in MOFs molding for compact form like making pellets requisite for industrial application (Chapman et al., 2009). Chemical stability has been considerably more rationalized than thermal and mechanical stability. However, there are a few key factors that should be highlighted. MOFs with excellent thermal stability can be derived from chemical metal cations with stable oxidation state (commonly metal with trivalent oxidation state (Mouchaham et al., 2018)) and ligand including sulfates, phosphonates, or pyrazolates (Shimizu et al., 2009). Meanwhile, carboxylate and phenolates as ligands undergo rapid decarboxylation and oxidation at high temperatures. For mechanical stability, MOFs with minimized porosities and dense structures present high durability to mechanical stress (Redfern and Farha, 2019).

3. Current strategies of MOFs based materials for pesticide adsorption

3.1. MOF based materials and its modification

Table 1 summarizes the current study of MOF and its modification for pesticide adsorption. Fig. 5 present the chemical structures of several pesticides discussed in this review.

3.1.1. Pristine MOFs

MOF exhibits a large surface area, well-built pore structure, and structure tunability, providing high selectivity for pesticide adsorption. De Smedt et al. (2015) reported MOF-235 (Fe) present as the most attractive material for faster adsorption and good regeneration of bentazon, clopyralid, and isoproturon from water compared to zeolite,

activated carbon, and carbonaceous resin, but their adsorption capacity was vice versa. MOF-235 has been aided by the extra cationic framework, nitrogen-doped ligand, smaller particle size, microporous structure, high surface area, and lower affinity towards this pesticide, which attributed to satisfactory in terms of kinetic and reusability. However, the instability structure of MOF-235 in the aqueous phase inhibits the adsorbent utilization for long-term reusability (De Smedt et al., 2015).

Singh et al. (2021) synthesized 3-D MOF crystal calcium fumarate (CaFu) with higher porosity, stability, better surface area, and more accessible active functional sites. Fumaric acid as bidentate ligand with two oxygen atoms directly coordinated with calcium center produces mesoporous structure (15.23 nm), 2308.03 m^2/g surface area, and neutral-basic stability. The synthesized CaFu MOFs were able to remove 97.3 % with a maximum adsorption capacity of 467.23 mg/g within 70 min. The non-covalent interaction through electron donor between active groups (NO_2 and Cl) groups of imidacloprid molecules and hydroxyl groups and metal center (Ca^{2+}) on MOFs framework was suggested as the primary mechanism.

In the past few years, the series of MIL-53 (Al, Cr) acted as special adsorbents with breathing behavior upon guest molecules loading even though they were built based on microporous channels. Jung et al. (2013) manifest the adsorption superiority of flexible MIL-53 (Cr) against 2,4-D with accelerated adsorption (only one h), which is much faster and higher uptake capacity compared to activated carbon (AC) and USY zeolite. It is impressive that the adsorption of 2,4-D by MIL-53 (Cr) is favorable, especially at low concentrations in the solution. The author suggested that the electrostatic interaction and the π– π interaction are dominant mechanisms for 2,4-D removal based on pH, temperature, thermodynamic and framework evaluation (Jung et al., 2013). Patil et al. (2011) reported the influence of pore-filling or breathing behavior on the nitrobenzene (NB) adsorption by MIL-53 (Al). MIL-53 (Al) adopted narrow pore (np) conformation with 1107.21 A^3 cell volume after activation. The phase transition to large pore (lp) occurred after loading NB up to 24/75 mg with 1256.76 Å3 cell volume higher than pristine material. Indeed, the breathing behavior significantly improved nitrobenzene adsorption with up to 3 and 6 ~ time higher capacity from zeolites and organoclays, respectively. Other mechanisms such as hydrophobic and π– π interaction also responsible for the adsorption improvement (Patil et al., 2011).

Xie et al. (2014) reported the presence of Al-O-Al and μ_2-OH in MIL-68 (Al) and CAU-1 benefit for NB adsorption. As a metal center, Al has relatively enhanced the electrostatic interaction of MOFs compared to Cr and V, attributed to the relatively higher partial charge metal cluster. Meanwhile, the textural properties (e.g., surface area, pore-volume, and pore size) are also crucial for NB removal. Even though CAU-1 has other NH2 groups as active sites, MIL-68 (Al) presents a higher surface area and pore size, with a higher adsorption capacity of 1130 mg/g compared to 970 mg/g of CAU-1 (Xie et al., 2014).

Abdelhameed et al. (2019) reported that two isostructural ZIFs MOF adsorbent, ZIF-8 (Zn) and ZIF-67 (Co), are efficient for prothiofos and ethion removal. The existence of prothiofos and ethion insecticides interaction with metal ions (P = S····Zn/Co) and hydrogen bonds formation with imidazolium (−>P = S···· H_{imid}) mainly determined as the mechanism of the insecticides adsorption The results demonstrated ZIF-8 (Zn) has higher adsorption capacity for prothiofons and ethion compared to ZIF-67 (Co) (ZIF-8: 367 and 296 mg/g; ZIF-67: 261 and 211 mg/g). Both ZIFs present a higher adsorption capacity of prothiofons rather than ethion which is attributed to the lower adsorption energy required based on isosteric heat calculation. Meanwhile, theoretical calculation revealed the distance of prothiofos, and ethion with Zn metal ions (−>P=S····Zn; 2.1 A^o) is shorter than Co (metal ions) and (−>P=S····Co; 3A^o) which provide stronger interaction and leads to higher adsorption capacity (Abdelhameed et al., 2019). Two ZIFs MOF adsorbents also can be reported as suitable adsorbents for boric acid removal (Lyu et al., 2017; Zhang et al., 2019a). Lyu et al. (2017) mentioned that the ZIF-8 exhibits a relatively high adsorption capacity of 247.44 mg/g at 45 °C for boron removal with excellent reusability. Meanwhile, Zhang et al. (2019a) reported that the ZIF-67 (Co) could provide loading capacity for boron up to 392.52 mg/g at 35 °C, which is much higher than ZIF-8. The author stated two major reasons for these phenomena: (1). The unsaturated electron configuration of Co as a metal source provides an easier way to coordinate with the adsorbent than Zn; (2). ZIF-67 has longer cell lengths and a greater cell volume than ZIF-8, indicating that the bigger pore size is more favorable to adsorbent entry and that the pore capacity of ZIF-67 can contain more adsorbents.

Water and chemical stable MOFs with exceptional surface area, UIO-66, have been introduced for methylchlorophenoxypropionic acid (MCPP) adsorption. Seo et al. (2015) unveiled the maximum uptake capacity of UIO-66 (370 mg/g) against MCPP, which is superior to activated carbon (303 mg/g). Compared with AC, the adsorption capacity is significantly high (7.5 times) at the low initial concentration (1 mg/L), while the kinetics constant ~ 30 times higher indicated that the adsorption reached equilibrium much faster. Electrostatic and π–π interactions was the feasible adsorption mechanism for MCPP adsorption based on the effect of pH on zeta potential and the adsorption (Seo et al., 2015).

Improving pesticide adsorption on pristine MOFs is mainly present in two strategic ways: ligand extension and defect strategies. The idea of ligand extension technique by expanding the pore width using a larger ligand. A super tetrahedron structure with mesoporous was created by coordinating the terephthalate ligand and trimeric chromium (III) octahedral. Mesoporous MIL-101 (Cr) was demonstrated as an adsorbent in a fixed bed system for continuous adsorption of diazinon. Mirsoleimani-azizi et al. (2018) reported that 92.5% of diazinon removal at 150 mg/L of initial diazinon concentration were achieved with MIL-101 (Cr). The mesoporous structure of MIL-101 (Cr) promoted the diffusion of large pesticide molecules towards porous structures (Mirsoleimani-azizi et al., 2018).

Jamali et al. (2019) performed Dichlorvos and Metrifonate adsorption with UIO-67 (2400 m^2/g), which has a broader pore aperture and larger surface area than UIO-66 (1500 m^2/g) owing to the use of lengthening linker 4,4-biphenyl dicarboxylic acid (BPDC) (Jamali et al., 2019). In terms of removal efficiency, UIO-67 exhibits remarkable performance compared to UIO-66. A larger surface area and more abundant Zr-OH groups contributed to the rapid and efficient removal of both insecticides by UIO-67. The chemical complexing or coordination mechanism between Zr-OH and phosphorus groups in insecticide appeared to be the primary mechanism on both MOFs. The experimental FTIR data supported the chemisorption suggestion. By comparing the surface charge of UIO and the adsorption capacity with pH variation, the electrostatic interaction has no significant influence on the adsorption (Jamali et al., 2019). In another study, Zhu et al. (2015) revealed that chemisorption contributes to glyphosate and glufosinate as two representative pesticides for UIO-67. The experimental FT-IR and XPS spectrum suggested that the reactive sites of the Zr-nodes, including Zr-OH and m3-OH, contribute strong affinity towards pesticides to form Zr-OH-P coordination, boosted by the existence of a missing linker. As a result, the maximum calculated adsorption capacity was 537 mg/g for glyphosate and 360 mg/g for glufosinate. The presence of methyl groups on glufosinate resulted in weaker interaction between adsorbate and Zr-OH in UIO-67, which ascribed to the higher capacity of glyphosate than glufosinate adsorption (Zhu et al., 2015).

Pankajakshan et al. (2018) designed two Zr-based MOFs adsorbents (UIO-67 and NU-1000) for glyphosate elimination through aqueous media adsorption. They studied the influence on adsorption uptake by varying the particle sizes of NU-1000 and UiO-67 (100–2000 nm). Due to the efficacy diffusion of glyphosate, the maximum adsorption uptake was reached with the smallest MOF nanoparticles (100–200 nm, i.e., 1517 and 1336 mg/g for NU-1000 and UiO-67, respectively). The interaction between the Zr node and glyphosate is shown by the altered binding energy of Zr-OH_2, Zr-OH, and Zr-O-Zr bonds in XPS spectra indicated the glyphosate adsorption. The Zr-O-P distance in NU-1000

(4.2) was less than in UiO-67 (4.6) based on theoretical calculations in line with the glyphosate capacity for two Zr MOFs (Pankajakshan et al., 2018).

Akpinar and Yazaydin (2018) studied the performance of water-stable MOFs such as ZIF-8, UIO-66, and UIO-67 on the atrazine adsorption as herbicide representative. As evaluated, the pore aperture and size affected the adsorption rate and capacity. Because of their narrower pore apertures, ZIF-8 and UiO-66 adsorbed significantly less atrazine than UiO-67. Meanwhile, UiO-67 demonstrated efficient adsorption and rapid adsorption performance within 40 min. Their large pore size and pore apertures permit the facile diffusion of adsorbates towards the framework. They observed that controlling the pH had no significant influence on the adsorption capacity of ZIF-8, UiO-66, UiO-67 since atrazine occurs in the neutral form in aqueous media. As evaluated, the hydrophobic and π–π interactions were responsible for the adsorption mechanism rather than the electrostatic interaction (Akpinar and Yazaydin, 2018).

The defect strategy was introduced to enlarge the porosity structures to enhance the accessibility active side on smaller apertures and pore size of MOFs. Clark et al. (2019) introduced defects into UIO-66 by controlling the amount of HCl (%vol) as the modulator. They demonstrated significant improvement in PFOS adsorption, up to ~ six times greater in adsorption capacity than a defect-free of UIO-66 (UIO-66-DF). The UIO-66-DF has an insufficient porous structure ($6A^{o}$) to accommodate a larger molecule of PFOS (diagonal dimension ~ $16A^{O}$). Meanwhile, the inaugurated defect structure provides a larger pore (~16 and ~20 Å) within the framework, which is crucial to proliferate the adsorption capacity due to larger internal surface area and the more significant number of coordinatively sites unsaturated Zr to coordinate with the PFOS head groups. An adequate modulator of up to 10% vol of HCl produced a suitable adsorbent with enough hierarchical porous structure. Adding up to 25% (v/v) of HCl generates a more significant number of defective sites that increase hydrophilic characteristics, while the hydrophobic interaction was suggested as one of the vital mechanisms. However, exaggerated addition of up to 50% of HCl generated a denser framework which limited the adsorption accessibility. The author suggests that 10% of HCl modulators were suitable for generating defect UIO-66 to provide multiple mechanisms such as acid-base complexation, electrostatic interaction, and hydrophobic interaction for PFOS adsorption (Clark et al., 2019).

Besides adding a modulator, the crystal defectivity can be generated through heatless synthesis or mild crystallization conditions, which may have been too soft to maintain in situ structural self-correction during framework construction. Charge imbalance or additional pore space, both desired to improve host–guest interaction, are known to be endowed by crystal defects (Ren et al., 2017). Tan and Foo (2021) created MIL-100 (Fe) through a water-based heatless synthesis technique. The MIL-100 (Fe)-heatless has a greater adsorption rate and capacity than HF-synthesized MIL-100 (Fe). The author underlined that the different capping agents such as F^{-}, Cl^{-} and OH^{-} on the coordination sphere of Fe (III) trinuclear cluster influence the surface charge characteristic. The existence of terminal hydroxide ions is more susceptible to protonation in the aqueous medium, resulting in a higher isoelectric point of MIL-100 Fe-heatless for better electrostatic interaction than fluoride ions HF-MIL-100 (Fe). Besides the electrostatic interaction, the Lewis base mechanism assisted by structural irregularities of MIL-100 (Fe), hierarchical micro- and mesoporosity, substantial internal surface area (~2000 m^2/g), and addition pore space were favorable for 2,4-D molecules adsorption (Tan and Foo, 2021).

The previous studies summarized that the accessibility of active sites is one of the crucial parameters to enhance the adsorption system by introducing mesoporous structure on the MOFs framework. In another study, the different morphological structures can influence the accessibility of the active site. A study by Xiao et al. (2021) introduces two different forms of nanomaterials, such as nanosheets and bulk crystal of MOFs, through interaction between Aluminum (Al) and tetrakis (4-carboxyphenyl) porphyrin ligand with the addition of cetyltrimethylammonium bromide (CTAB). The adsorption performance exhibit Al-TCPP nanosheets have better chlorantraniliprole adsorption capacity (371.91 mg/g) than the bulk crystals (222.11 mg/g). The Al-TCPP nanosheets present versatility on the hierarchical formation of the porous structure by creating stack up layer by layer, which provides a higher surface area than Al-TCPP bulk crystals. In addition, The as-synthesized nanosheet also manifests excellent hydrophilic characteristics and water stability, which benefit aqueous medium adsorption (Xiao et al., 2021).

In conclusion, the pristine MOFs themselves have shown good performance against pesticide removal from aqueous solutions. However, we must pay attention to the ligand and metal selection and their synthesis methodology, which is crucial for acquiring MOFs with adequate adsorption sites and porosity. Such defective strategy and shaped morphology (e.g, nanosheets) are well-performed to refine the accessibility of the active site and exploit the MOFs channel for better pollutants diffusion.

3.1.2. *Functionalization of metal-organic framework*

The functionalization of pristine MOFs has been confirmed as an effective way to enhance adsorption performances. Post modification and ligand functionalization are two promising strategies so far. A study from Abdelhameed et al. (2021b) investigated the adsorption performance on amine-modified MIL-53 (Al) (Al-$(BDC)_x(BDC\text{-}NH_2)_{1-x}$, x = 0.00, 0.25, 0.50, 0.75, and 1.00) for dimethoate as pesticide representative. The different amino ratios were synthesized through one-pot synthesis comprising aluminum as the metal center and different ligand ratios of BDC and NH_2-BDC. Two crucial parameters have been evaluated as the significant contributor to the adsorption performance, such as adsorption energies and surface area of MOFs. The hydrogen bond formation between phosphate oxygen and MOFs amine hydrogen and intramolecular interaction between sulfur groups on pesticide and amine hydrogel was reported as the major mechanism. Indeed, the increasing amino ratio would overcome the energy configuration required for hydrogen bonding (H). However, this behavior was opposite to the experimental performance on dimethoate adsorption capacities of amino-functionalized MIL-53 (Al). The result reveals a ratio of 1:1 BDC: NH_2BDC ligand provide MOFs [Al-(BDC)0.5(BDC-NH2)0.5] with the highest adsorption capacity and highest surface area. [Al-(BDC) 0.5(BDC-NH2)0.5] had a maximum adsorption capacity of 513.4 mg /g, which was significantly higher than that of free amino Al-BDC (154.8 mg g1) and full amino Al-BDC-NH2 (266.9 mg g1).

Currently, post-modification MOFs introduced cationic sites towards UIO-66 via quaternary amine anionic-exchange incorporation (UiO-66 (Zr)- NMe^{3+}). The-as synthesized MOFs demonstrate excellent adsorption performance compared to amine-modified MOFs and pristine MOFs (UIO-66-NH_2 and UIO-66, respectively). As evaluated, the adsorption capacity of 2,4-D followed the order of UIO-66-NMe^{3+} (279 mg/g), UIO-66-NH_2 (222 mg/g) > UIO-66 (179 mg/g), but the order of surface area is reversed. All MOFs and their modifications exhibit electrostatic interactions (e^{-}) and π–π conjugation as the primary mechanism. However, the addition mechanism such as cation-π bonding and the ion exchange and stronger electrostatic interaction sites contributed to the higher adsorption capacity of UIO-66-NMe^{3+} (Wu et al., 2020).

Meanwhile, Hasan et al. (2013) investigated the post-modification of MIL-101 (Cr) with Aminomethane sulfonic acid (AMSA) and ethylenediamine (ED). The additional acidic (SO_3H) and basic groups (NH_2) active sites were generated by coordinating unsaturated metal sites and amino groups substances from AMSA and ED. As evaluated, the maximum adsorption capacity was following the order of ED-MIL-101 > MIL-101 > AMSA-MIL-101 for clofibric acid adsorption. ED-MIL–101 exhibits the highest performance on the clofibric acid due to acid-base interaction between basic adsorbent and acidic adsorbate, resulting in a 1.17 higher maximum adsorption capacity than pristine MIL-101 (Hasan et al., 2013).

In another study, two strategic approaches were subjected to functionalize MIL-101 (Cr) for glyphosate adsorption. The first strategy is the incorporation of amino groups (–NH_2) on MIL-101 (Cr) via one-pot synthesis comprising of NH_2-BDC (amino terephthalic acid) and Chromium while the second strategy is post-modification of material synthesized from the first strategy through urea addition (UR_2-MIL-101 Cr). The adsorption performance for NH_2-MIL-101 (Cr) was better than the urea functionalized MIL-101 (Cr). The limited urea functionalized MIL-101 (Cr) performance was caused by steric hindrance. The electrostatic interaction was mainly involved in the adsorption mechanism of both adsorbents (Feng and Xia, 2018). MIL-101 (Cr) also can be modified with furan or thiophene derivatives. The as-synthesized materials ameliorated the performance of pristine MIL-101 (Cr) for diuron (DUR), alachlor (ALA), tebuthiuron, and gramoxone, which ascribed by the π–π stacking and hydrogen bonding interaction (Yang et al., 2019).

Conclusively, the presence of the bridging ligands on MOFs offers the active center by inaugurating the functional organic sites free from MOFs framework construction, which can perform as either acid or base active sites. A diversity of organic functional groups, such as alcohols, amides, amines, carboxylates, and pyridine, can provide active acidic or basic sites for electrostatic interaction and hydrogen bonding. Meanwhile, These diverse functional groups are usually bound to the organic ligand before MOFs construction, but also the addition of functional groups was conducted by the grafting method during post-modification. It is worth noting that the selection MOFs with good chemical, thermal and mechanical stability as a host material is crucial for the adsorption based on post-modification based MOFs since the functional groups came from substances with the strong character of either acid or base compound. These drawbacks can usually be overcome by using an already modified ligand prior to MOFs synthesis.

3.1.3. MOF based composite

Through synergistic effects among components with rationally specified characteristics, MOFs coupled with other functional materials can significantly improve adsorption performance compared to individual substances. Graphene oxide (GO) has been used for MOFs adsorbent modification due to its porous framework and abundant functional groups. For instance, Yang et al. (2017) prepared nanocomposite through in-situ growth synthesis of UIO-67 (Zr) on the graphene oxide surface (UIO-67/GO). UIO-67/GO exhibits excellent performance on the GP adsorption with maximum adsorption capacity reaching 483 mg/g, which is higher than other GO-based adsorbents. The adsorption enhancement was contributed by the Zr-OH groups of UIO-67 (Zr) on the GO surface through Zr-O-P coordination and the large surface area and the availability –OH and –COOH groups of GO.

Adsorption practicality is also influenced by the recovery and regeneration of the adsorbent after its utilization. As a result, scientists have created various solutions to this challenge, including magnetic derivative materials for facile separation of adsorbent using an external magnetic field. Due to its magnetic characteristics, Fe_3O_4 is frequently employed in magnetic MOFs. Yang et al. (2018) prepared hybrid magnetic material (Fe_3O_4@SiO_2@UIO-67(Zr) through a layer-by-layer assembly method and subsequently used it for glyphosate adsorption. The prepared adsorbent exhibits satisfactory performance on adsorption with high adsorption capacity (257 mg/g) and regeneration capability up to four times. The adsorbent provides Zr-OH functionalities for the interaction of phosphate groups with additional magnetic core Fe3O4 to assist the adsorption process. In addition, XRD patterns revealed that excellent water stability and no-significant structure were altered after the glyphosate adsorption, indicating the reusability stability (Yang et al., 2018).

The magnetic MOFs can also modify by adding functional groups such as layered double hydroxides. The abundant functional group provides many affinity sites for pesticides adsorption and modification. Lu et al. (2021) successfully attached the double-layer hydroxide (Zn-Al-LDH) and MIL-53 towards the Fe_3O_4 shell to create a mesoporous structure (5.2 nm) and relatively high surface area (726.1 m^2/g) for fungicides adsorbent. The-as synthesized composite exhibits a relatively rapid equilibrium time with only 5 min to achieve 43.54 and 71.71 mg/g adsorption capacity for triadimefon and epoxiconazole (Lu et al., 2021). In addition, the XPS spectrum revealed the shifted energy bonding of –OH groups and C=O and C=C groups in the used-adsorbent indicate the hydrogen bonding and π–π interaction was the primary mechanism for the adsorption.

A study by Li et al. (2020b) evaluated the adsorption performance of a double-layer structure with polyhedron morphology of M−ZIF−8@ZIF-67. Using a single layer Fe3O4-ZIF-8 as the magnetic core and a layer of ZIF-67 as the outer layer, a novel metal–organic framework (M−ZIF−8@ZIF-67) was effectively constructed for fipronil and its derivatives removal via adsorption. The-as synthesized adsorbent exhibits remarkable performance with up to 99.7% removal of fipronil from water owing to its homogenous porous structure, which improves the adsorption and organic pollutants removal (Li et al., 2020b).

Magnetic Walled Carbon Nanotubes (MWCNTs) are considered advanced materials that exhibit outstanding properties which can be used as support for MOFs. Liu et al. (2018) construct hybrid magnetic composite (M−M−ZIF−8) through coordination polymerization of ZIF-8 deposited on the MWCNTs surface. The integration was found to be effective for eight pesticides removal (triazophos, diazinon, phosalone, profenofos, methidathion, ethoprop, sulfotep, and isazofos) from soil and water via adsorption. The authors stated that valence-electron-driven adsorption is the possible mechanism in which the organophosphorus pesticide molecules share or exchange electrons with the empty active sites of M−M−ZIF−8 (Liu et al., 2018).

Recently, polysaccharide-based MOFs composites have drawn considerable attention owing to their biocompatibility and mechanical strength. Moreover, the structural flexibility, tunable porosity, and high surface area make the composite more valuable (Nadar et al., 2019). For instance, the combination of cyclodextrin and MOFs offer an intrinsic cavity for organic molecules inclusion. In another study, Liu et al. (2017) assembled magnetic nanocomposite through the integration of Cu–benzene-1,3,5-tricarboxylate (BTC) and iron oxide-GO-β-cyclodextrin (Fe_3O_4-GO-β-CD) (Liu et al., 2017). Because of its high surface area and hydrophobic inner pore, this composite efficiently removed various neonicotinoid pesticides (thiamethoxam, imidacloprid, acetamiprid, nitenpyram, dinotefuran, clothianidin, and thiacloprid) from water. The presence of N-containing groups, hydrophobic groups, and delocalized electrons from the benzene rings or five-membered heterocycles in the adsorbate molecules resulted in hydrogen bonding, hydrophobic interactions, electrostatic interaction, and π– stacking interactions, which were interpreted as adsorption mechanisms for the seven pesticides.

Incorporating functional chitosan/chitin into MOF-based biomaterials provides aided properties such as hierarchical porosity and structural robustness. Hydroxy and acetamido groups with the three-dimension fibrous network can act as a suitable matrix for MOF immobilization through electrostatic interaction and hydrogen bonding. Huang et al. (2020) studied the effect of doping ratio of UIO-66 on the on ionic liquid (IL)-modified chitosan (ILCS) ILCS/U-X (X represents the ratio of UiO-66). The addition of UIO-66 increases the oxygen content by providing abundant carboxyl groups, which provide more reactive sites for adsorption for 2,4-D adsorption. Meanwhile, the existence of free amino groups assists the hydrogen bonding between 2,4-D and composite. ILCS/U-10 has the best doping ratio as an adsorbent to achieve a maximum adsorption capacity of 262.9 mg/g for 2,4-D removal within 60 min of adsorption from an aqueous solution. Electrostatic interaction has the most significant impact on the adsorption since the interaction between anionic 2,4-D and cationic composite significantly reduced after the pH was altered from the optimal range (Huang et al., 2020)

In a recent study, Liang et al. (2021) developed MOF modified aerogel (MOF@MCPA) through crosslinking of MOF@PWCNTs composite, chitosan, and glutaraldehyde. MOF@PWCNTs composite itself was constructed by in-situ growth of ZIF-8 or UIO-66-NH_2 on the surface of

polydopamine-modified carboxyl-terminated multi-walled carbon nanotubes (PCMWCNTs) (Liang et al., 2021). Both composite exhibit outstanding hydrophilicity, thermal stability, light weight, and mechanical resistance properties. For the adsorption performance, the UIO-66-NH_2@MCPA has better versatility on the adsorption performance for ionic (chipton) and non-ionic herbicide (alachlor) removal, while ZIF-8@MCPA was unable to remove the non-ionic herbicide (alachlor) effectively. However, both composite manifest good adsorption performance compared to single MOFs (UIO-66 and ZIF-8). The exposed active sites on the composite surface were ascribed to the adsorption of CHI or ALA molecules, in which large pores at the micron level of MPCA enabled the fast adsorption of the pesticides and expedited the interaction between MOF nanoparticles and pesticides. The electrostatically driven mechanism was responsible for chipton adsorption, while hydrogen bonding and p- p were primary mechanisms for alachlor removal.

The most abundant natural polysaccharide, cellulose, is also a promising candidate for MOFs composite. Hydroxyl groups on cellulose can facilitate the chemical modification that assists MOF immobilization on the cellulose surface. The cellulose provides several refined characteristics such as hydrophilicity, biodegradability, low density, and significantly larger surface area than the pristine MOFs. In addition, the coordination versatility aided structural robustness for environmental implementation (Kim et al., 2019). Abdelhameed et al. (2016) evaluated the performance of Cu-BTC@Cotton composite on the removal of ethion from aqueous solution. The composite bestows promising performance by removing 97% of ethion, and maximum adsorption capacity reached 182 mg/g while maintaining its performance even after five cycles of regeneration. There are two crucial factors involved in this adsorption: (i) The coordination bond between Cu atom in MOFs and S atom of ethion; (ii) the availability of hydroxyl groups of cellulose for hydrogen bonding with ethion. The composite also manifests potential application for selective pesticide adsorption such as dicamba, 4- chlorophenoxy-acetic acid, 2,4-D, and 2-(2,4-dichloro phenoxy) propionic acid in packed column (Abdelhameed et al., 2016).

The same research groups designed macroporous membrane cellulose acetate (112.6 ± 30.1–496.0 ± 23.7 nm), and subsequently, the Cu-BTC were in-situ growth within the porous membrane. The practicability of the prepared membrane was used for dimethoate removal through adsorption. The addition of 40% Cu-BTC content on the porous membrane significantly increased the adsorption performance corresponding to the surface area elevation. Meanwhile, over 40% of Cu-BTC would decline the adsorption performance, which correlated to the decrease of the surface area caused by pore-blockage. The authors suggested the electrostatic interaction, hydrogen bonding, and the porous structure and functional groups coordination provoked the dimethoate adsorption onto a membrane (Abdelhameed et al., 2021a).

Another organic material, such as protein, can refine the adsorption ability of the metal–organic framework. Namdar Sheikhi et al. (2021) create multifunctional hybrid bovine serum albumin (BSA)-metal–organic framework (BSA/PCN-222(Fe)) composite for methyl parathion and diazinon adsorption. The merits properties of PCN-222 (Fe) and BSA provide multiple bunding such of functional groups such as amino, thiol, and carboxylic acid groups assisted by their mesoporous structures (pores size 2.73 and 1.09 nm), which facilitate the mass transfer of the interaction of pesticide towards functional groups of composite via hydrogen bonding, hydrophobic interactions, π–π stacking interactions, van der Waals forces, electrostatic interactions, acid-base interactions (only for diazinon), and adsorption onto coordinatively unsaturated Zr^{4+} and Lewis Fe^{+3} sites. Combining these materials provides a maximum adsorption capacity of 370.4 mg/g and 400 mg/g for methyl parathion and diazinon, respectively, within only 3 min adsorption time (Namdar Sheikhi et al., 2021).

In summary, MOFs-based composite design has been proven as a superior adsorbent with high performance compared to pristine and functionalized MOFs. The incorporation of MOFs towards inorganic or organic matrix possesses active sites improvement, better dispersity while also improving the porosity and stability of the adsorbent.

3.1.4. MOF derived materials

Because of their high specific surface area, versatile porous structure, and ease of production, MOF-derived nanoporous carbon (NPC) and carbon hybrid materials have piqued attention in recent years for pollutants removal (Yu et al., 2021). The pyrolyzed carbon material can be a metal-containing material, or metal can be removed to create a metal-free adsorbent, depending on the functionality and application (Chen et al., 2018). The presence of metal can enhance the active sites of the adsorbent, and the integration with other functional material throughout pyrolysis generate material with more functionalities and multiple mechanism possibility. For instance, Abdelillah Ali Elhussein et al. (2018) prepared CeO_2 nanofibers through Ce-BTC MOF calcination and afterward was utilized for 2,4-D removal. Micro/nano-rod structured adsorbents provide maximum adsorption capacity (95.78 mg/g) within two h through electrostatic interaction and π–π stacking interactions between 2,4-D and CeO_2 surfaces. However, particle aggregation was observed when a high amount of adsorbent was used, which diminished the surface area and lengthened the diffusion path (Abdelillah Ali Elhussein et al., 2018). A study by Bhadra et al. (2020) assembled highly porous carbon (CDM-74) through carbonization of MOF-74. They reported the adsorbent could acquire up to 340 mg/g uptake capacity with four times regeneration for DEET removal, which is ascribed by the mesoporous structure and high acidity content. High acid content is required to provide or donor hydrogen atom towards DEET as hydrogen acceptor. Hydrogen bonding, van der walls, and electrostatic interaction were put forwards as the primary driving force mechanism with DEET (Bhadra et al., 2020). In another study, Liu et al. (2019a) synthesized multifunctional porous carbon (β-CD MOF-NPC) through high-temperature pyrolysis of β-cyclodextrin MOF. Before carbonization, β-cyclodextrin MOF (β-CD MOF) was fabricated through β-cyclodextrin as ligand and potassium benzoate as the metal center. The prepared materials provide a high surface area with microporous structure and rich potassium content for effective removal of amide herbicides via π–π interaction, hydrogen bond, and electrostatic interaction.

Chen et al. (2017) fabricated the core–shell structure of magnetic porous carbon-based sorbent ($ZnO/ZnFe_2O_4$) through Fe^{III} modified MOF-5 followed by pyrolysis. Subsequently, the as-synthesized material was used for atrazine adsorption (Chen et al., 2017). The adsorbent contains a high content of oxygen functional groups suitable for hydrogen bonding with OH, NH_2, or NH groups of atrazine and hydrophobic interaction. Ahmed et al. (2017) synthesized porous carbon with high nitrogen content through MOF calcination after incorporating ionic liquid onto ZIF-8 (IMDC). The nitrogen content was controlled by IL doping content and pyrolysis temperature. Afterward, the IMDC was exerted on aqueous medium atrazine and diuron adsorption. They observed that IMDC has a higher uptake capacity of atrazine (208 mg/g) than activated carbon and ZIF-8. The atrazine and diuron adsorption were primarily controlled by hydrogen bonding since atrazine act as hydrogen donor and diuron as hydrogen acceptor while nitrogen provides a good merge for hydrogen interaction (Ahmed et al., 2017). Meanwhile, Sarker et al. (2017) reported that IMDC was a suitable adsorbent for diuron and 2,4-D removal. The experimental result validated that the adsorption capacities reached 284 and 448 mg/g, respectively, and the adsorption was mainly controlled through hydrogen bonding, hydrophobic interaction and, π–π stacking interactions (Sarker et al., 2017).

In this study, MOFs-derived materials have provided remarkable performance with versatile utilization against varios pesticides since they provide various adsorption driving forces such as hydrogen bonding, π-πinteraction, and hydrophobic interaction that may vary depending on the environmental parameters. Furthermore, their large surface area and hierarchical porous structure with controllable

Table 2
Mathematical equations of isotherm, kinetic, and thermodynamic.

Isotherm Adsorption Modelling				
Model Approaches	**Non-Linear Equation**	**Linear Equation**	**Parameters**	**Design (Y vs X axis)**
Henry	$q_e = k_{HE}\, C_e$	–	k_{HE} = Henry isotherm model constant (L/g)	C_e vs q_e
Langmuir	$q_e = \frac{q_{m,L} K_L C_e}{1 + K_L C_e}$	$\frac{C_e}{q_e} = \frac{1}{K_L q_m} + \frac{C_e}{q_m}$ $\frac{1}{q_e} = \frac{1}{q_m} + \frac{1}{q_m K_L C_e}$ $q_e = q_m \frac{q_e}{K_L C_e}$ $\frac{q_e}{C_e} = K_L\, q_m - K_L\, q_e$	$q_{m,L}$ = Langmuir maximum sorption capacity (mg/g) K_L = Langmuir Affinity Constant (L/mg)	$\frac{C_e}{q_e}$ vs C_e $\frac{1}{q_e}$ vs $\frac{1}{C_e}$ q_e vs $\frac{q_e}{C_e}$ $\frac{q_e}{C_e}$ vs q_e
Freundlich	$q_e = K_F\, Ce^{1/n}$	$\log q_e = \log K_F + \frac{1}{n} \log C_e$	K_F (mg/g)(L/g)^n : Freundlich isotherm constant related to the adsorption capacity n ($1 < n < 10$): Degree adsorption favorability	$\log q_e$ vs $\log C_e$
Dubinin-Raduskevich (DR)	$q_e = q_{m,DR} \exp[-k_{DR}\, \varepsilon_{DR}{}^2]$ $\varepsilon_{DR} = RT\,(1 + \frac{1}{C_e})$	$\ln q_e = \ln q_{m,DR} - k_{DR}\, \varepsilon_{DR}{}^2$	$q_{m,DR}$ = DR maximum sorption capacity (mg/g) ε = Polanyi Potential (kJ/mol) k_{DR}=adsorption energy constant (mol^2/kJ^2)	$\ln q_e$ vs ε
Dubinin-Astakhov (DA)	$q_e = q_{m,DA} \exp[-(\varepsilon_{DA}/E_{DA})^n]$ $\varepsilon = RT \ln (C_s/C_e)$	$\ln q_e = \ln q_{m,DA} - (\varepsilon/E_{DA})^n$	$q_{m,DA}$ = DA maximum sorption capacity (mg/g) ε = adsorption potential (kJ/mol) n = Fitting Parameter based DA E_{DA} = Characteristic energy of adsorption (kJ/mol) C_e = equilibrium concentration (mg/L) C_s = Adsorbate maximum solubility (mg/L)	$\ln q_e$ vs ε
Temkin	$q_e = \frac{RT}{b_T} \ln K_T\, C_e$	$q_e \frac{RT}{b_T} \ln K_T + \frac{RT}{b_T} \ln C_e$	b_T = Temkin sorption heat constant (J/mol) K_T (L/mg): Temkin isotherm equilibrium binding constant	q_e vs ln Ce
Sips	$q_e = \frac{q_{m,SP} K_{SP} C_e^{n_{SP}}}{1 + K_{SP} C_e^{n_{SP}}}$	$\ln\left(\frac{q_e}{q_{m,SP-}q_e}\right) = \frac{1}{n} \ln C_e + \ln (K_{SP})^{1/n}$	K_S (L/mg): Sips isotherm model constant q_{ns} (mg/g): Sips isotherm maximum adsorption capacity n_S: Sips isotherm model exponent	$\ln\left(\frac{q_e}{q_{m,SP-}q_e}\right)$ vs $\ln C_e$
Toth	$Q_e = \frac{Q_{m,To} K_{TO} C_e}{\left(1 + K_{TO} C_e^{n_{To}}\right)^{1/n_{To}}}$	$\ln\left(\frac{q_e}{q_{m,SP-}q_e}\right) = n \ln C_e + n \ln (K_{SP})^1$	$Q_{m,To}$ (mg/g): maximum adsorption capacity K_{To} (L/mg): Toth isotherm constant n_{To} : Toth isotherm model exponent	$\ln\left(\frac{q_e}{q_{m,SP-}q_e}\right)$ vs $\ln C_e$
Redlich-Peterson (R-P)	$Qe = \frac{K_{RP} C_e}{1 + \alpha_{RP} C_e^g}$	$\ln\left(\frac{K_{RP} C_e}{q_e}\right) = g \ln C_e + \ln \alpha_{RP}$	K_{RP} (L/g): Redlich-Peterson isotherm constant α_{RP} (1/mg): Redlich-Peterson isotherm constant g ($0 < g < 1$): Redlich-Peterson isotherm binding constant	$\ln\left(\frac{K_{RP} C_e}{q_e}\right)$ vs $\ln C_e$
Kinetic Adsorption Modelling				
Model Approaches	**Non-Linear Equation**	**Linear Equation**	**Parameters**	**Design (Y vs X axis)**
Pseudo First Order (PFO)	$q_t = q_{e,cal}\,(1 - e^{k_1 t})$	$\ln (q_e - q_t) = \ln q_e - k_1 t$	Q_t (mg/g): adsorption capacity at various time t $Q_{e,cal}$ (mg/g): calculated equilibrium capacity of adsorption k_1(1/min): the rate constant of PFO kinetic model	$\ln (q_e - q_t)$ vs t
Pseudo Second Order (PSO)	$q_t = \frac{Qe^2, cal\, k_2 t}{1 + Q_e, cal\, k_2 t}$	$\frac{t}{q_t} = \frac{1}{k_2 q_e^2} + \frac{t}{q_e}$	$Q_{e,cal}$ (mg/g): calculated equilibrium adsorption capacity k_2(g/mg.min): the rate constant of PSO kinetic model h (mg/g.min) = $Q^2_{e,cal}\, k_2$: the initial adsorption rate	$\frac{t}{q_t}$ vs t
Elovich	$q_t = \frac{ln(1 + (\alpha\beta t))}{\beta}$	$q_t = \frac{1}{\beta} \ln (\alpha\beta) + \frac{1}{\beta} \ln (t)$	α(mg/g.min): the initial adsorption rate β(g/mg): a parameter related to the activation energy for chemisorption and extent of surface coverage	q_t vs ln t
Intra-Particle Diffusion (IPD)	$Q_t = k_{IPD}\, t^{0.5} + C$	–	k_{IPD} (mg/g.min$^{0.5}$): IPD constant rate C (mg/g): a constant that provide value regarding to thickness of the boundary layer.	q_t vs $t^{0.5}$
Thermodynamic Adsorption Modelling				
Gibbs Energy	$\Delta G = -$ R.T. ln ($K_e{}^0$)	–	$K^0{}_e$ = equilibrium constant (dimensionless	–
Vant-Hoff	$K_e{}^0 = \exp\left(\frac{\Delta S^0}{R} - \frac{\Delta H^0}{RT}\right)$	$\ln (K_e{}^0) = \frac{\Delta S^0}{R} - \frac{\Delta H^0}{RT}$	$K^0{}_e$ = equilibrium constant (dimensionless) ΔS^0 = Entropy at reference state (J/mol) ΔH^0 = Enthalpy at references state (J/mol.K)	ln ($K_e{}^0$) vs $\frac{1}{T}$
Equlibrium Constant (Based Langmuir Model)	$K_e{}^0 = 55.5 \times 1000 \times K_L$	–	K_L = Langmuir binding affinity (L/mg)	–
	$K_e{}^0 = 10^6 \times K_L$	–		–
	$K_e{}^0 = 55.5 \times 1000 \times M_W \times K_L$	–	M_w = Molecular weight of adsorbate (g/mol) K_L = Langmuir binding affinity (L/mg)	–
Equlibrium Constant (Based Freundlich Model)	$K_e{}^0 = \frac{K_f x \rho}{1000}\, x \left(\frac{10^6}{\rho}\right)^{(1 - \frac{1}{n})}$	–	K_F = Freundlich Constant (mg/g)(L/g)^n n ($1 < n < 10$): Degree adsorption favorability ρ = Density of water (1 g/ml)	–
Equlibrium Constant (Based on Best Fitted Constant Model)	$K_e{}^0 = \frac{K_g .1000 . M_W . [adsorbate]^0}{\gamma}$	–	$[adsorbate]^0$ = standard concentration of adsorbate (1 mol/L) K_g = best fitted isotherm model constant (L/mg) Mw = molecular weight of adsorbate (g/g/mol)	
		–		

(*continued on next page*)

Table 2 (*continued*)

Isotherm Adsorption Modelling				
Model Approaches	**Non-Linear Equation**	**Linear Equation**	**Parameters**	**Design (Y vs X axis)**
Equlibrium Constant (Based on based on partition model)	$K_e^0 = K_p = \frac{C_s}{C_e}$		C_s = adsorbed adsorbate concentration (mg/L) C_e = equilibrium concentration of adsorbate (mg/L)	K_p as slope of graphing ln (C_s/C_e) vs C_s as y and × axis and extended the C_s value to zero
Equlibrium Constant (Based on distribution coefficient)	$K_e^0 = K_d = \frac{q_e}{C_e}$	–	q_e = equlbrium adsorbed adsorbate (mg/g) C_e = equilibrium concentration of adsorbate (mg/L)	K_d as slope of graphing ln (Q_e/C_e) vs C_e as y and × axis and extended the C_e value to zero

morphology have successfully assisted the pollutants diffusion towards MOFs. Nevertheless, several challenges should be addressed shortly, such as metal leaching, low density and aggregation of metal nanoparticles while their synthesis methods are also complex, which limited the applicability for adsorption.

3.2. The summary of mathematical model for pesticide adsorption based MOFs

Isotherm, kinetic, and thermodynamic adsorption modeling with its parameters were crucial for determining the adsorption mechanism and assessing the practicability of the designed adsorbent for industrial application. Here, we summarize the mathematical equation of isotherm, kinetic and thermodynamic (Table 2) with the brief study case of pesticides based Metal-Organic Framework Adsorption.

3.2.1. Isotherm adsorption

Reliable adsorption equilibrium data are essential for efficient adsorption process design. Adsorption isotherms are mathematical representations of adsorption equilibrium. The adsorption isotherm model described the mechanism of interaction pollutants and adsorbents by evaluating the data and adsorption properties. Several adsorption isotherm equations originally established for gas-phase adsorption are used to describe the adsorption equilibrium data of various pesticide types by various types of MOFs. These equations are either one parameter model (henry), two-parameter models (Langmuir, Freundlich, Dubinin-Radushkevich (D-R), Temkin) or three-parameter models (Sips, Toth, and Redlich-Paterson). A detailed explanation of isotherm mathematical equations has been presented elsewhere (Al-Ghouti and Da'ana, 2020).

Table 1 summarizes the isotherm model used to interpret the pesticide adsorption by MOFs. Henry's isotherm model is the simplest adsorption isotherm model since the partial pressure of the adsorptive gas is proportional to the amount of surface adsorbate. This isotherm model presents a good fit to adsorbate adsorption at low concentrations, in which all adsorbate molecules are isolated from their nearest neighbors (Ayawei et al., 2017). Henry isotherm model has rarely been used to describe the adsorption model for pesticide removal using MOF, but a few studies reported that the henry isotherm model could fit data well (Lyu et al., 2017; Zhang et al., 2019a).

Langmuir and Freundlich isotherm equations are the most frequently used to describe the isotherm model. However, the Langmuir model tends to interpret the pesticide adsorption more frequently than the Freundlich model in several cases, which indicates the heterogeneity of the MOFs surface. MOFs modification had a substantial impact on the materials' adsorption ability. Because more functional groups from modifying agents were attached to the surface of MOFs, and the surface became heterogeneous, it may usually improve the adsorption capacity of the adsorbents. Therefore, several MOFs modifications follow the Freundlich model, which indicates the possibility of multilayer adsorption with different adsorption energy in each active site. In certain situations, both models can describe the same isotherm data of pesticide adsorption (Clark et al., 2019; Abdelillah Ali Elhussein et al., 2018; Feng and Xia, 2018). For instance, Clark et al. (2019) reported that both the Langmuir and Freundlich isotherm models match the equilibrium data for the defective UiO-66 materials well. The strong correlation values for the Langmuir isotherm fit indicate that PFOS adsorbs monolayer on defective UiO-66. According to the Freundlich fitting, this adsorption may happen on various sites with different adsorption energies.

Several less frequent isotherm equation models such as Temkin, Dubinin Astakhov, Redlich-Peterson, and Sips have simulated the pesticides adsorption data for a few MOFs. Initially, the Temkin isotherm was used for determining the chemisorption of hydrogen gas on platinum electrodes in acidic solutions. In most systems, the Temkin model is failed to describe the experimental adsorption. Even though some studies reported the occurrence of chemisorption through metal or ligand coordination, physical bonding is the primary controlled mechanism. Huang et al. (2020) reported that the Temkin model was suitable for the 2,4-D adsorption on ILCS/U-10. However, their study revealed that physical interactions such as hydrogen bonding and electrostatic interaction controlled the adsorption (Huang et al., 2020). Therefore, the result should be re-validated to find a suitable adsorption model. In some reviews, the Temkin isotherm model has also highlighted its failure to describe the complex adsorption of the liquid phase (Al-Ghouti and Da'ana, 2020; Foo and Hameed, 2010). Another isotherm model, the Dubinin-Astakhov equation, was derived based on Polanyi theory to describe adsorption on the microporous structure of the adsorbent. This equation was beneficial to determine the distribution energy of atrazine adsorption on non-homogenous microporous structure ZnO/$ZnFe_2O_4$. Redlich Peterson and sips model are hybrid isotherm model that features Freundlich and Langmuir isotherm models with three parameters. Both models can demonstrate the heterogeneity system of MIL-53 (Al) and CeO_2 (Abdelillah Ali Elhussein et al., 2018).

3.2.2. Kinetic adsorption model

For the appropriate design of an adsorption system, the ability to identify sorption kinetics for a particular substance is critical. As a result, numerous sorption kinetic models for diverse adsorption kinetic systems have been created and validated. Interfacial kinetics, shrinking core concept, and intraparticle surface diffusion theory were the primary ideas used to construct the present adsorption kinetic models. Specific equations and theoretical concepts of kinetic models have been reviewed elsewhere (Qiu et al., 2009). The pseudo-first-order and pseudo-second-order equations are the most often used models to describe the kinetics of pesticide adsorption onto MOF and its modification. Briefly, The PFO model assumes that the adsorbate's adsorption kinetic rate is proportional to the difference between equilibrium and adsorption capacity in the system. The PSO model is based on the notion that chemisorption is an adsorption rate-controlling step in which the adsorbate and the adsorbent share electrons or transfer electrons.

Table 1 shows that the PSO model is the most often utilized kinetic model for pesticide adsorption by MOFs, and only a few adsorptions kinetic systems follow the pseudo-first-order. Compared to the pseudo-second-order equation, the pseudo-first-order equation rarely represents kinetic data adequately. As a result, chemisorption is the primary control mechanism in the adsorption of MOFs as an adsorbent, and the bonding between adsorbate molecules and the surface functional groups in MOF plays a significant role in the process. However, mostly MOFs publications rarely investigate the influence of temperature on isotherm adsorption or kinetic models. Therefore, it is too early to mention

Table 3
Thermodynamic studies on pesticide adsorption onto MOFs and its modification.

Materials	Targeted Pesticides	T (°C)	Δ G° (kJ/mol)	Δ S° (kJ/mol.K)	Δ H° (kJ/mol)	Ref.
MIL-53 (Cr)	2,4-D	25	−24.9			(Jung et al., 2013)
		30	−25.1	41.6	−12.5	
		35	−25.4			
Fe_3O_4@ZnAl-LDH@MIL-53(Al)	TDF	25	−0.483	0.047	−13.530	(Lu et al., 2021)
		35	−0.953			
	EXZ	25	−5.525	0.065	−13.855	
		35	−6.178			
MIL-100 (Fe)	2,4-D	30	− 2.157	3.775	−1.019	(Tan and Foo, 2021)
		45	− 2.233			
		60	− 2.270			
ZIF-8	BA	25	−8.1323	0.07449	14.0390	(Lyu et al., 2017)
		35	−8.9969			
		45	−9.6168			
ZIF-8@MPCA	CPT	30	−2.473			(Liang et al., 2021)
		40	−3.008	42.81	10.46	
		50	−3.325			
	ALC	30	−0.399			
		40	−2.019	157.03	47.16	
		50	−3.537			
ZIF-67	BA	25	–12.68	–0.06	–31.39	(Zhang et al., 2019a)
		35	–12.17			
		45	–11.42			
UIO-66	DHV	30	2.3437			(Jamali et al., 2019)
		40	2.4865	−28.56	−6.31	
		50	2.6293			
	MTF	30	3.4693			
		40	3.5928	−26.47	−4.56	
		50	3.7251			
	2,4-D	25	−19.65	−32.36	−29.33	(Wu et al., 2020)
		35	−19.45			
		45	−18.99			
UIO-66-NH_2	2,4-D	25	−20.56	−59.63	−38.28	(Wu et al., 2020)
		35	−19.85			
		45	−19.35			
UIO-66-NH_2@MPCA	CPT	30	−4.989			(Liang et al., 2021)
		40	−5.739	63.57	14.24	
		50	−6.256			
	ALC	30	−0.804			
		40	−2.545	186.89	55.86	
		50	−4.548			
UIO-66-NMe^{3+}	2,4-D	25	−23.87	−67.57	−43.94	(Wu et al., 2020)
		35	−22.98			
		45	−22.53			
ILCS/U-10	2,4-D	25	6.86			(Huang et al., 2020)
		30	7.01	−27.12	−1.206	
		35	7.16			
UIO-67	DHV	30	1.6438			(Jamali et al., 2019)
		40	1.8119	–33.61	−8.54	
		50	1.9799			
	MTF	30	1.7536			
		40	1.9063	−30.54	−7.50	
		50	2.0590			

chemisorption as the controlling factor in the adsorption process. Few investigations have identified inconsistencies between the control mechanisms indicated by equilibrium and kinetic data interpretation. The adsorption was discovered to be regulated by a chemisorption process based on the interpretation using pseudo-first and pseudo-second-order models. However, a visual depiction of the adsorption equilibrium data reveals a process that was the opposite of chemisorption: the adsorbent's adsorption capacity decreased as the temperature increased (Abdelillah Ali Elhussein et al., 2018; Huang et al., 2020; Patil et al., 2011; Tan and Foo, 2021; Yang et al., 2018). These two kinetic models cannot be used to identify the mechanism of the adsorption process in the case of opposite mechanisms obtained from the interpretation of both adsorption equilibria and kinetic data because they plot kinetic data independently regardless of the physisorption or chemisorption mechanism in the adsorption process.

Plazinski et al. (2009) reviewed that PSO can represent kinetic data in which intraparticle diffusion is the limiting rate step despite the fundamental derivative chemisorption on PSO (Plazinski et al., 2009). As mentioned earlier, the adsorption process consists of three stages of phenomena: (1) boundary layer diffusion: solute transfer from the bulk liquid phase to the adsorbent's exterior surface via the boundary layer, (2) solute transfer from the exterior surface to the binding sites are called intraparticle diffusion, (3) surface reaction: the solute molecules form chemical or physical interactions with the surface binding sites. In summary, a few pesticides adsorption onto MOFs and their modification primarily controlled by multiple adsorption mechanisms, either boundary layer diffusion more dominant than intraparticle diffusion or vice versa (Feng and Xia, 2018; Lyu et al., 2017; Singh et al., 2021; Tan and Foo, 2021; Yang et al., 2017; Zhang et al., 2019a; Zhu et al., 2015).

3.2.3. *Thermodynamic model*

Thermodynamic parameters give further information about the intrinsic energy changes during adsorption. Gibb's free energy change (ΔG°), standard enthalpy change (ΔH°), and standard entropy change (ΔS°) are three thermodynamic parameters used to estimate the performance of the adsorption process. Van Hoff's model is usually used to

acquire these parameters from the adsorption equilibrium data. Further detailed thermodynamic evaluation and model have been reviewed elsewhere (Anastopoulos and Kyzas, 2016; Lima et al., 2019). Table 3. highlights the thermodynamics parameters of pesticide adsorption on MOFs and their modification. Δ S^o positive presents increasing randomness at the solid-solution interfaces during pesticide adsorption; meanwhile, Δ S^o negative indicates a decrease in randomness due to the association between pesticides and MOFs. As a result, the amount of pesticides on the MOFs decrease progressively.

Most of the thermodynamic data show that as temperature rises, the value of ΔG° decreases, which indicates that the adsorption process appears to be more spontaneous and thermodynamically viable at higher temperatures due to the mobility of molecules and the adsorbate affinity. However, several studies found the reverse tendency, suggesting that as the temperature rises, the amount of pesticides adsorbed on the surface of MOFs decreases, which indicates that adsorption is more feasible at lower temperatures. The negative ΔH^o indicates that the adsorption of pesticides onto MOFs is an exothermic process, while positive ΔH^o the adsorption process is endothermic.

Commonly, Adsorption refers to the spontaneous and exothermic reaction. For validation, the adsorbed ions–molecules have fewer degrees of freedom than the aqueous state, leading to entropy value depletion during adsorption (Bansal and Goyal, 2005). The exothermic reaction occurs when the total energy release in bond coordination between adsorbate and adsorbent is higher than absorbed energy during bond breaking. The possible explanation for the endothermicity adsorption is the occurrence of the adsorbed solvent molecules desorption followed by the adsorbate moieties adsorption (Saha and Chowdhury, 2011). This theory is feasible to validate the nature of the endothermic phenomenon of MOFs since the metal cluster in the framework are coordinated with solvent or host–guest molecules (Li et al., 2016a). Therefore, the pesticides molecules should replace more than one molecule of solvent to be coordinated with MOFs active sites. This statement is also supported by the positive ΔS^o value, which indicates the displacement of adsorbate solvent molecules with pesticide molecules. These phenomena would increase the net translational entropy, which influences the thermodynamics system randomness (Saha and Chowdhury, 2011).

The value of ΔG° may provide insight into the sorption type, either physisorption or chemisorption. Physisorption is characteristic with ΔG° magnitudes ranging from −20 to 0 kJ/mol, while chemisorption ranges from −80 to −400 kJ/mol. In addition, the multilayer adsorption was also determined through the value of the standard free energy change ranging from less than zero kJ/mol and >20 kJ/mol. The sorption mechanism also can be determined based on the magnitude of ΔH°. Physical adsorption produces heat of the same order of magnitude as condensation, ranging from 2.1 to 20.9 kJ/mol, whereas chemisorption produces heat in the range of 80–200 kJ/mol (Anastopoulos and Kyzas, 2016). According to the free Gibbs energy and enthalpy criteria, it is evident that most pesticides adsorption systems are controlled either by physisorption or physisorption enhanced by chemisorption.

3.3. Influenced aspect for pesticides adsorption onto MOFs and its modification

3.3.1. pH

The adsorbent's surface charge, the degree of protonation of the adsorbate molecule, and the degree of dissociation of the functional group on the active site of the adsorbent are all affected by the solution's initial pH. Jung et al. (2013) investigated the removal efficiency of MIL-53 towards 2,4-D pesticide in a pH range of 2–10. 2,4-D adsorption on MIL-53 was favored on the pH solution ranging 3–5 since the isoelectric point of MIL-53 is five while the pKa value of 2,4-D is around 2.7–2.8. Therefore, the optimum pH for maximum removal was 2.8 to achieve strong electrostatic interaction between positive charged MIL-53 and negatively charged 2,4-D (Jung et al., 2013).

Seo et al. (2015) reported that the surface charge of UIO-66 provides a more positive charge by decreasing the pH solution. At a pH 4–5.5, the adsorption of MCPP was higher, but the MOFs charged became more negative when the pH increased, which caused electrostatic repulsion between MOFs and pesticides (Seo et al., 2015). In another study, pH selection for optimum adsorption should also be determined based on material stability. For instance, Singh et al. (2021) selected pH 6.5 for IDP adsorption by calcium fumarate MOFs. When the pH value was turned to acidic medium (pH 2–5) and slightly base solution, the 3-D MOF coordination was destructed due to metal oxide formation of Ca^{2+} and deprotonation of fumaric ligand.

In conclusion, different pesticides and MOFs behave differently with pH. Moreover, stable MOFs at a particular pH provide greater adsorption capacity, in which neutral pH is also preferred. For detailed conspectus study of the chemical stability of several MOFs has been highlighted elsewhere (Moumen et al., 2021).

3.3.2. Effect of co-existence impurities

Pollutants such as Ions (Akpinar et al., 2019; Clark et al., 2019; Jamali et al., 2019; Li et al., 2020a; Lu et al., 2021; Tan and Foo, 2021; Wu et al., 2020; Zhu et al., 2015) and other organic pollutants (phenoxy carboxylic acid and herbicides) (Huang et al., 2020) can be found in industrial and municipal wastewater. As a result, the coexistence of these pollutants has a significant impact on the feasibility of the adsorption process. The co-existence of ions provides two significant impacts on the adsorption phenomenon, such as organic pollutants solubility adjustment and interfering with the electrostatic interaction owing to the screening/shielding effect (Zhang et al., 2019b). Wu et al. (2020) found that the different ions affected the adsorption performance of UiO-66(Zr)- NMe3. They reported that the monovalent ions (Cl^-; OH^-) have facile accessibility to occupied reaction sites on the adsorbent surface, which interferes with the electrostatic interaction between adsorbent and 2,4-D. Meanwhile, SO_4^{2-} is more difficult to swiftly access the quaternary amine groups owing to the tetrahedral shape of UiO-66-NMe^{3+}. In another study, Clark et al. (2019) reported that the SO_4^{2-} and Cr (IV) ions notably disturbed the PFOS adsorption while the Cl^- ions had a negligible effect on the PFOS adsorption (Clark et al., 2019). A similar phenomenon also has been observed by Tan and Foo (2021). They revealed that the existence of Na_2SO_4 significantly reduced the adsorption performance of MIL-100 (Fe) compared to NaCl at the same salinity concentration and adsorbent dosage. The MIL-100 (Fe) had sulfate oxygen atoms, which are more favorable to interact with sulfate ions than chloride ions (Tan and Foo, 2021). However, several studies reported that several salts solution such as NaCl, $NaNO_3$, Na_2SO_4, $CaCl_2$, $MgSO_4$, KNO_3, and NaOAC and various metal ions such as Fe^{3+}, Fe^{2+}, Ca^{2+}, Na^+, Zn^{2+}, K^+, Al^{3+}, and Mg^{2+} had the negligible effect of deteriorating of MOFs adsorption selectivity (Akpinar et al., 2019; Li et al., 2020a). Moreover, adding up to 4% NaCl in an aqueous solution would increase the ionic strength and solubility of azole fungicides, improving the adsorption performance of Fe_3O_4@ZnAl-LDH@MIL-53(Al) (Lu et al., 2021).

The presence of other herbicides pollutants such as phenoxy carboxylic pesticides (MCPA and 2,4-D), diuron, and bentazone could decrease the adsorption selectivity of MOFs. A study by Huang et al. (2020) discovered that ILCS/U-10 has high selectivity adsorption for phenoxy carboxylic acid herbicides than other herbicides, which is indicated by the more significant reduction of 2,4-D adsorption with the increasing MCPA concentration. Meanwhile, It was observed that the presence of diuron and bentazone had negligible deterioration on MOFs performance for 2,4-D adsorption (Huang et al., 2020)

3.3.3. Desorption, regeneration, and stability

Regeneration and desorption study is crucial in determining the long-term commercial feasibility of a functionalized adsorbent. There are two types of regeneration techniques: physical and chemical regeneration. Chemical regeneration employs a chemical solvent to

Table 4
Regeneration performances of MOFs and its modification for pesticides adsorption.

Types of MOFs	Targeted Pesticides	Regenerant	Cycle	Adsorbed Pollutants (% or mg/g)		References
				Fresh Samples	Recycled Materials	
IMDC	DUR	Ethanol	4	284 mg/g	176.2 mg/g	(Sarker et al., 2017)
IMDC	2,4-D	Ethanol	4	448 mg/g	333.2 mg/g	
ZIF-8	BA	Water	5	247.4 mg/g	~87 mg/g	(Lyu et al., 2017)
ZIF-67 (Co)	BA	HCl	5	579.80 mg/g	94.1% (of the original capacity)	(Zhang et al., 2019a)
MIL-53 (Al)	2,4-D	Water/Ethanol (1:1)	3	556 mg/g	494.8 mg/g	(Jung et al., 2013)
MIL-100 (Fe)	2,4-D	Ethanol	5	858.11 mg/g	80% (of the original capacity)	(Tan and Foo, 2021)
		Acetone		858.11 mg.g	40% (of the original capacity)	
UIO-66	MCPP	Water/Ethanol	3	370 mg/g	142 mg/g	(Seo et al., 2015)
UIO-66-NH_2	2,4-D	Ethanol	3	72.99 mg/g	30.7 mg/g	(Li et al., 2020a)
		Acetone			6.8 mg/g	
		Methanol			39.5 mg/g	
		Acetonitrile			24.7 mg/g	
		Dichloromethane			28.4 mg/g	
Fe_3O_4@ZnAl-LDH@MIL-53 (Al)	TDF	Water and Methanol	5	~99%	88%	(Lu et al., 2021)
	EXZ			~99%	98%	
ILCS/U-10	2,4-D	Water/Ethanol (3:7)	6	246 mg/g	212.6 mg/g	(Huang et al., 2020)
CDM-74	DEET	Acetone	4	340 mg/g	239.88 mg/g	(Bhadra et al., 2020)
UIO-67	ATZ	Acetone	3	~29 mg/g	27 mg/g	(Akpinar and Yazaydin, 2018)
NU-1000 (Zr)	ATZ	Acetone	3	~98%	92%	(Akpinar et al., 2019)
IMDC	ATZ	Ethanol	4	208 mg/g	161.5 mg/g	(Ahmed et al., 2017)
Cu-BTC@Cotton	ETH	Acetonitrile	5	97%	85%	(Abdelhameed et al., 2016)
ZIF-8	ETH	Acetonitrile	5	366.7	227.5 mg/g	(Abdelhameed et al., 2019)
	PTH			279.3	282.62 mg/g	
ZIF-67	ETH			261.1	152.5 mg/g	
	PTH			210.8	192.7 mg/g	
BSA/PCN-222 (Fe)	MPRT	Acetonitrile	1	Not-mentioned	97.8%	(Namdar Sheikhi et al., 2021)
			12		78.7%	
		Ethanol	1		91.8%	
		Methanol	1		89.4%	
	DZ	Acetonitrile	1		98.6%	
			12		79.2%	
		Ethanol	1		92.6%	
		Methanol	1		89%	

eliminate adsorbate from the solid adsorbent, whereas physical regeneration uses heat energy. Table 4 presents the current studies of desorption and regeneration of MOFs after pesticides adsorption. Desorption entails removing connections between pesticides molecules and the adsorbent's active site while retaining the adsorbent's physical and chemical characteristics (Li et al., 2020c). To date, no physical regeneration has been carried out to recover the MOFs adsorbent. Most studies of regeneration of MOFs after pesticides adsorption utilized chemical-based regeneration such as organic solvents, distilled water, and acid. Several organic solvents such as methanol, ethanol, acetone, and acetonitrile are the most common organic solvent used for the pesticide's elimination from the surface of MOFs due to facilely soluble and excellent interaction with pesticides substances. For instance, acetone was selected for NU-1000 regeneration since the adsorbed atrazine has a high solubility in acetone (Akpinar et al., 2019). Namdar Sheikhi et al. (2021) reported that acetonitrile was more effective among other solvents (ethanol and acetone) to maintain the adsorption performance of saturated BSA/PCN-222 (Fe) after five consecutive cycles (Namdar Sheikhi et al., 2021). In addition, they also stated that the desorption time and eluent volume and the addition of ultrasonic irradiation are also involved in desorption efficiency adjustment.

Meanwhile, Li et al. (2020a) revealed that methanol was the most effective solvent for regeneration of UIO-66-NH_2 after 2,4-D adsorption (Li et al., 2020a). In another study, Tan and Foo (2021) reported that more polar organic solvent provides more desorption ability to remove adsorbed 2,4-D. Therefore, ethanol was more preferred than acetone-based solvent for regenerating adsorbents loaded with pesticides (Tan and Foo, 2021).

The pH of the solvents also plays a crucial role in the desorption process. The solvent's pH alters the adsorbent's surface charge, weakening the electrostatic interaction between adsorbate molecules and adsorbents. Singh et al. (2021) utilized dilute HCl (pH 5.5) to regenerate CaFu MOFs after imidacloprid adsorption (Singh et al., 2021). In several studies, water or combination water and organic solvent can also detach the adsorbed pesticide molecules from the adsorbent through certain time agitation. Meantime, ultrasonic irradiation combined with organic solvent treatment can also desorb molecules from the adsorbent surface. The ultrasonic irradiation facilely destructs the non-covalent interaction between adsorbate and adsorbent while the addition solvent dissolves the pesticides molecules from adsorbent (Tan and Foo, 2021). Adsorbent stability is also a critical factor in its commercial application; the destruction of the adsorbent structure during the adsorption will lead to secondary contamination and make recycling the material more difficult. In summary, most research studies revealed no evidence that leads to framework destruction after and before regeneration (based on PXRD and FTIR analysis), which indicates outstanding stability of metal–organic framework (Table 4). However, Lyu et al. (2017) reported that water stability was the main problem of ZIF-8 regeneration; however, ZIF-8 still maintains its high adsorption performance against boric acid owing to the greater porous structure and surface area (Lyu et al., 2017).

In a nutshell, the desorption performance has highly influenced the characteristic of adsorbent, adsorbate, and particularly solvent. A suitable solvent was vitally required to increase the exterior driver force to rapidly diffuse the pollutants from the surface and porous of adsorbent towards liquid phase while also weakening the interaction between adsorbent and adsorbate. Several factors should be considered for the successful desorption system: (1) the concentration differences of adsorbate in adsorbent and body liquid. The higher magnitude of differences may increase the mass transfer process and diffusion of pollutants from the adsorbent porous towards liquid-phase; (2)—the solubility and polarity between adsorbate and solvent. For instance, less polar solvents (e.g.acetone) were preferred for atrazine dissolution, while more polar solvents (e.g., ethanol) were suitable for the 2,4-D pollutants desorption. In this case, it is crucial to evaluate the value of

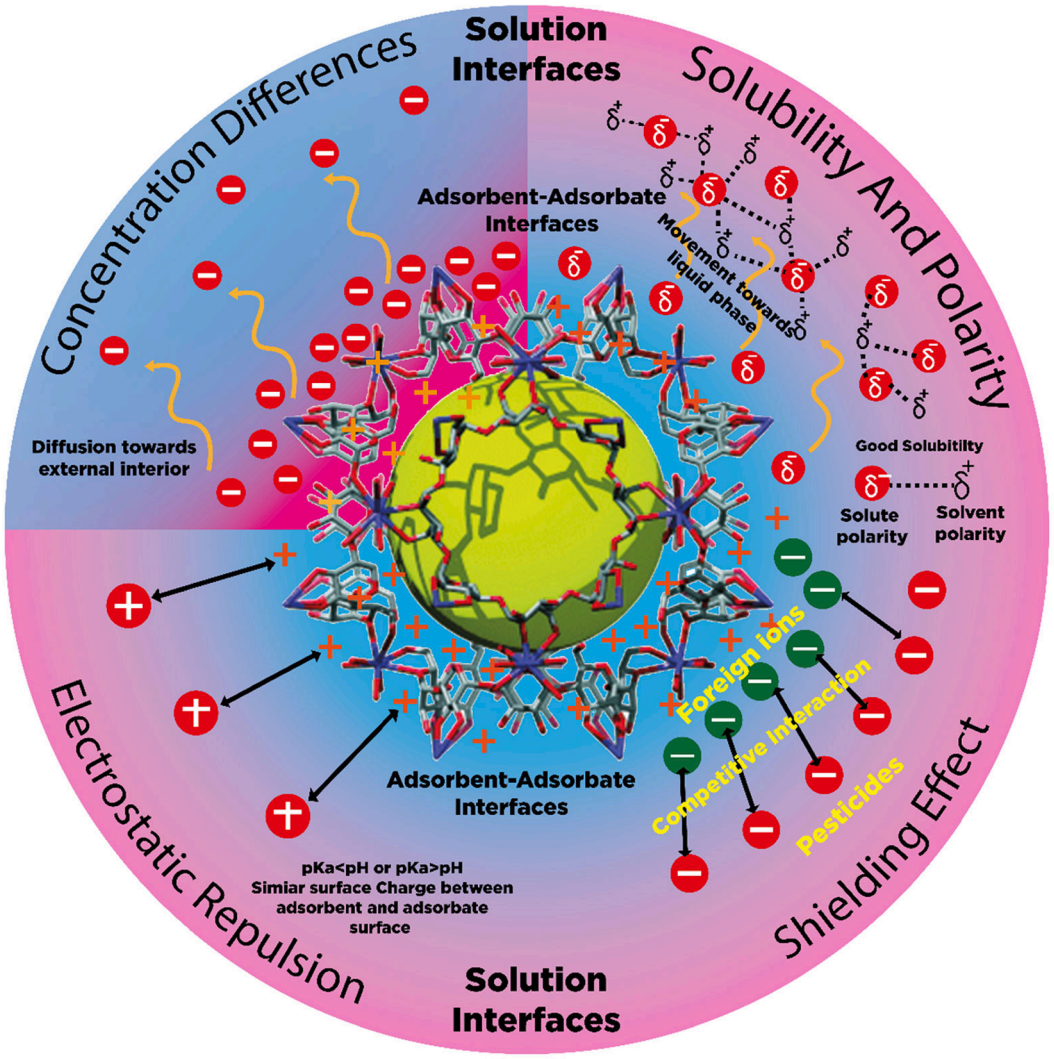

Fig. 6. Plausible mechanism of pesticides desorption from MOFs.

log K_{OW} (octanol/water partition coefficient) and the water solubility. When the value of Log K_{OW} is higher, then the solubility tendency of pesticides towards less-polar solvent is greater and vice versa. (3) Electrostatic interaction between pollutants and adsorbent. Weaken the electrostatic interaction through pH adjustment is the effective solution for achieving high desorption. In this desorption system, Analyzing the pKa of adsorbate and surface charge adsorbent while also evaluating the adsorption behavior of pollutants under various pH should be required. (4). The presence of co-existence pollutants or ions likes Na_2SO_4 may increase the desorption rate through electrostatic interaction interference by creating a screening/shielding effect. However, it is required to analyze which ions or pollutants are suitable for the desorption system since some of the ions may have a negligible effect or have the possibility to increase the solubility of pesticides and strengthen the electrostatic interaction. Apart from these fourth factors, the addition of ultrasonic irradiation, adjustment of extraction time and eluent volume, and finding MOFs with exceptional chemical, mechanical, and thermal stability would also significantly impact adsorbent recyclability. Fig. 6 presents the plausible mechanism of desorption mechanism of MOFs

4. Metal-organic framework (MOFs) design mechanism for pesticides adsorption

As summarized previously, the pathways comprise surface and pore adsorption aided with several mechanisms such as electrostatic interaction, hydrogen coordination, chemical bonding, acid-base interaction, and special features including hydrophobicity and breathing behavior, and defective structure.

Electrostatic interaction (e^-) is commonly observed throughout the pesticides adsorption between readily ionized adsorbate and the surface charged adsorbates. E^- can grant effective performance through repulsive and attraction interaction. As present in Fig. 7, the adsorption of 2,4-D towards MIL-100 (Fe), particularly at pH 3–4.3, could be described by e^- mechanism since the isoelectric point of MIL-100 (Fe) at 4.3. When the pH solution is $>$ 4.3, the e^- repulsion occurs due to a similar negative charge formed between adsorbent and adsorbate. Similarly, the adsorption phenomenon was observed for MCPP adsorption on UIO-66 (Zr). The optimum pH adsorption was approximately 4–5.5, which indicates the presence of e^- mechanism between negatively and positively charge of MCPP and UIO-66 Zr, respectively (Fig. 7 (d); (e); (f)). When the pH solution is over 7, the sorption capacity of UIO-66 deteriorates since the weakening electrostatic occur because both materials possess negatively charged materials. The existence of adsorption at pH $>$ 7 is contributed by the π–π interactions. These kinds of phenomena have been observed for 2,4-D adsorption and anionic pesticides with other adsorbents such as MIL-53 (Cr) (Jung et al., 2013), ZIF-67 (Co) (Zhang et al., 2019a), and IOO-66 (Zr) (Clark et al., 2019).

Besides the e^- interaction, the π–π interactions also became the

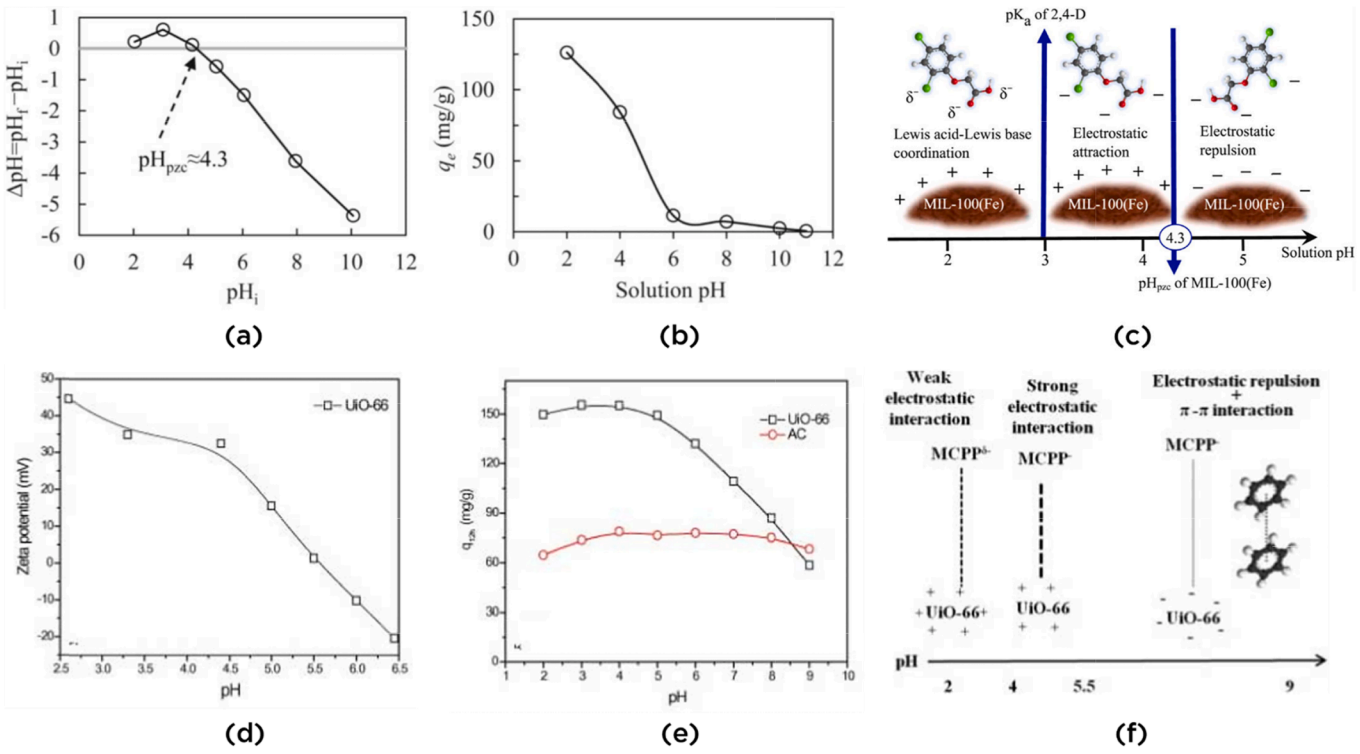

Fig. 7. (a). pH zero charge plot of MIL-100 (Fe); (b) Effect of pH solution on MIL-100 (Fe) adsorption; (c) Plausible mechanism of 2,4-D adsorption onto MIL-100 (Fe); this figure is reprinted with permission from (Tan and Foo, 2021). Copyright © 2021 Elsevier B.V. (d) Influence of pH on the equilibrium adsorbed adsorbate of MCPP on UIO-66 and activated carbon (C_o = 20 mg/L, 12 h); (e). pH effects on Zeta Potential of UIO-66; (f). A plausible mechanism of MCPP adsorption onto UIO-66; this figure is reprinted with permission from (Seo et al., 2015) from Copyright © 2015 Elsevier B.V.

possible approaches for pesticides adsorption since the pesticides and MOFs contain π- electrons (Jung et al., 2013; Patil et al., 2011; Mirsoleimani-azizi et al., 2018; Abdelhameed et al., 2019; Zhang et al., 2019a; Akpinar and Yazaydin, 2018; Seo et al., 2015; Akpinar et al., 2019; Li et al., 2020a; Wu et al., 2020; Hasan et al., 2013; Yang et al., 2019; Liang et al., 2021; Liu et al., 2017; Li et al., 2020b; Huang et al., 2020; Namdar Sheikhi et al., 2021; Lu et al., 2021; El-Hussein et al., 2018; Liu et al., 2019a; Sarker et al., 2017). Meanwhile, hydrogen bonding (H) is regularly evaluated as an efficient adsorption mechanism for pesticides removal sing MOFs-based adsorbents. The presence of hydrogen acceptor and donor position was crucial to increase the feasibility of pesticides adsorption. For instance, Bhadra et al. (2020) reported that the high acidic content of highly porous carbon (CDM-74) acted as donor hydrogen while DEET was a hydrogen acceptor. In another study, the IMDC was feasible to ATZ, DUR, and 2,4-D adsorption from aqueous solution through hydrogen bonding since the adsorbent behaves as both hydrogen donor and acceptor while DUR and 2,4-D act as hydrogen donors and ATR act as hydrogen donors. This adsorption mechanism was also observed for other MOFs based materials on pesticides removal (Abdelhameed et al., 2019; Abdelhameed et al., 2021b; Li et al., 2020a; Xie et al., 2014; Yang et al., 2019; Liang et al., 2021; Yang et al., 2017; Liu et al., 2017; Abdelhameed et al., 2021a; Huang et al., 2020; Namdar Sheikhi et al., 2021; Lu et al., 2021; Liu et al., 2019a; Ahmed et al., 2017; Sarker et al., 2017; Chen et al., 2017; Bhadra et al., 2020). Therefore, the π–π interactions and hydrogen bonding was vital adsorption mechanism for pesticides removal.

Compared to e^-, H and π–π interactions, acid-base interaction (ABI), hydrophobic (h), chemical bonding (c), and pore-filling (PF) are the unique mechanism for pesticides removal from the aqueous phase. For ABI interaction, the mechanism proceeded through the interaction of metal nodes and pesticides as lewis acid and base interaction (Clark et al., 2019, Pankajakshan et al., 2018, Hasan et al., 2013, Li et al., 2020b, Namdar Sheikhi et al., 2021). There is also the possibility of ABI interaction through Bronsted lewis acid and base interaction. However, the pre-arrangement of charged salts via ABI may be considered electrostatic interaction (Wu et al., 2020; Hasan et al., 2013). Hydrophobic (h) interaction required specific modification such as the incorporation of hydrophobic groups (e.g., CH_3) via post-synthesis, composite and MOF derived materials (Akpinar and Yazaydin, 2018; Liu et al., 2017; Namdar Sheikhi et al., 2021; Sarker et al., 2017; Chen et al., 2017). These approaches were effective in limiting the water molecules contact towards metal clusters. However, it has to be underlined that a strong hydrophobic surface is not always the solution since they exhibit problematic issues in the mass transfer process between solid and liquid phases.

Although pore filling (PF) has not progressively developed for pesticides adsorption, significant improvement has been shown for pesticides adsorption for specific MOFs. Exploiting larger pore structures provides better accessibility of active sites and diffusion of large molecules (Tan and Foo, 2021; Clark et al., 2019; Xiao et al., 2021; Abdelhameed et al., 2016; Namdar Sheikhi et al., 2021). While most of the previously mentioned mechanisms only involved the physical attraction, several designed MOFs possess chemical adsorption, which the adsorption occurs through valence sharing electron between MOFs metal cluster and pesticides (Mirsoleimani-azizi et al., 2018; Abdelhameed et al., 2019; Lyu et al., 2017; Zhang et al., 2019a; Jamali et al., 2019; Singh et al., 2021; Yang et al., 2017; Yang et al., 2018; Liu et al., 2018; Abdelhameed et al., 2016; Abdelhameed et al., 2021a; Lu et al., 2021).

From the previous studies, it can be inferred that the MOFs possess diverse morphological structures to provide a variety of mechanisms for pesticides removal. A combination mechanism is usually involved in justifying the adsorption possibility rather than a single mechanism. Fig. 8 exhibits a summary of pesticides adsorption using MOFs and their modification.

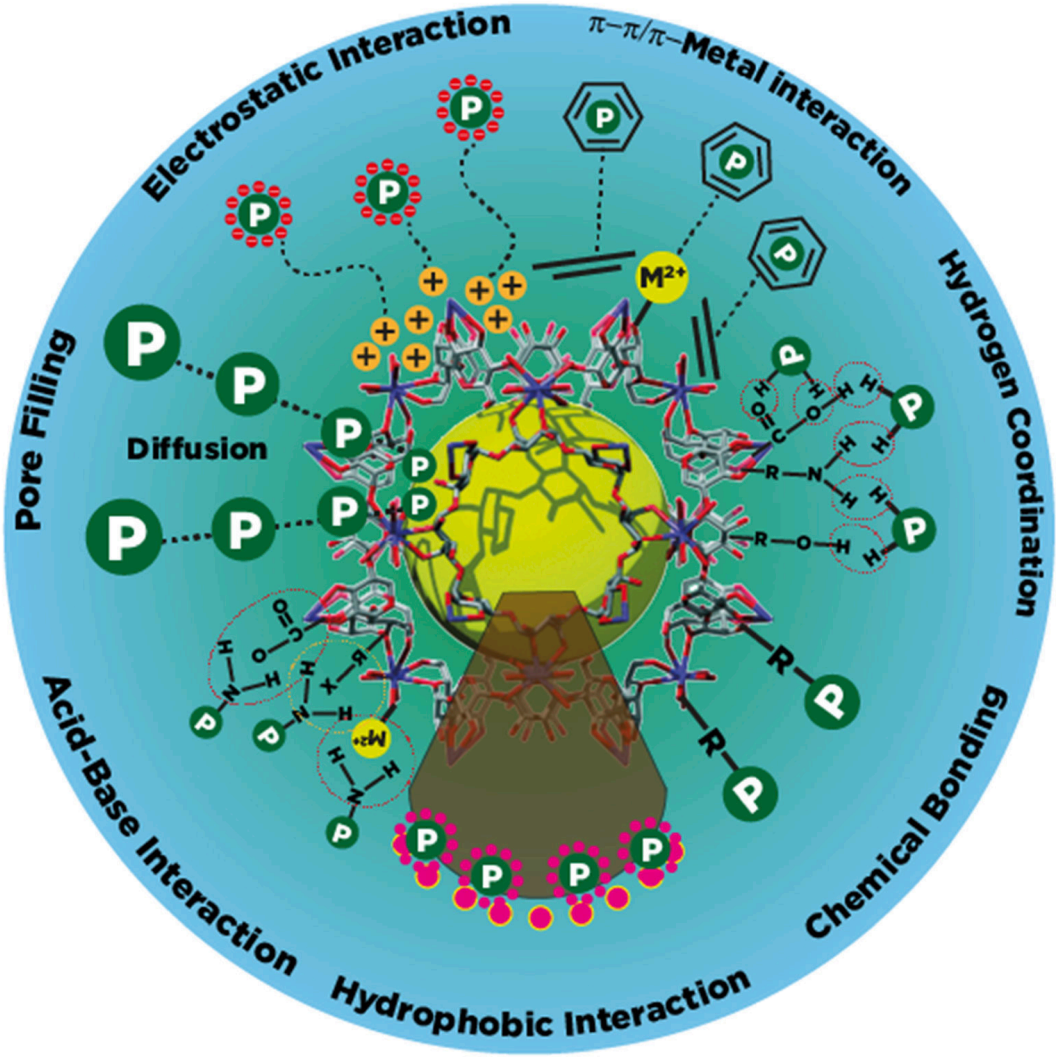

Fig. 8. Summary of adsorption mechanism for pesticides using MOFs as adsorbent.

5. Conclusion and future outlooks

MOFs are promising adsorbents for the future application of pesticides removal. Several strategies such as improving pore structure and addition functional groups through various functionalization (e.g., Ligand enlargement, composite material, and post-modification) have been revealed to be an efficient way to refine the adsorption performance and recoverability as stable of adsorbents. Besides the adsorbent characteristic, co-existence impurities and pH are particularly prominent to MOFs' selectivity and adsorption efficiency. Current studies have revealed that the selective uptake of pesticides adsorption by MOFs was controlled by various common mechanisms such as electrostatic interaction, hydrophobic interaction, π-π interaction, pore filling, acid-base interaction, and hydrogen-bond. Isotherm studies have indicated that most pesticides adsorption occurred through homogenous and monolayer adsorption, while a few studies of MOFs adsorption have shown the possibility of heterogeneous adsorption. The pseudo-second-order equations are considered the most applicable model to represent pesticides adsorption in kinetic modeling.

Although the research on the utilization of MOFs as adsorbents for pesticide removal is currently growing, the main issues impact the practical use of MOFs for pesticides removal. (1). Current studies offer promising outcomes on MOFs performance for pesticides removal. However, real wastewater's economic evaluation, reusability, and utilization are still scarce. All these factors are required before implementing MOFs as potential adsorbents for pesticide removal on an industrial scale. (2) Most studies only focused on single pesticide adsorption. The actual water bodies consist of multi-component substances with different environmental conditions. The adsorption mechanisms between single and multi-component systems are completely different. The competition for the adsorption sites between pesticides and other pollutants made the adsorption mechanism and selectivity unclear. (3). MOF-derived nanoporous carbon (NPC) and carbon hybrid materials are promising for adsorbents in chemical and physical characteristics. However, the study on applying these materials as adsorbents is scarce. Therefore, this effort should be put forwards to exploit MOFs derived materials for pesticides elimination; (4). Most highlighted MOFs and their modification manifest microporous structures prone to pore blockage or inaccessible active sites. Ligand extension technique and defect strategy are common ways to induce the mesoporous/macroporous structure to improve the accessibility of active sites, molecular diffusion, and mass transfer rate. Other preparations of engineered mesoporous/macroporous MOFs techniques include mixed ligand technique, templating or non-template synthesis, supercritical fluid synthesis, post-synthetic strategy, and stepwise ligand exchange (Guan et al., 2018), have well-developed which also give an excellent prospect to refine the ability of MOFs adsorption. MOFs and MOFs-derived materials not just have proven to be effective adsorbents but also as versatile materials with numerous possibilities in porosities and structural configuration for adsorption applications.

Declaration of Competing Interest

The authors declare that they have no known competing financial interests or personal relationships that could have appeared to influence the work reported in this paper.

Acknowledgments

This study was supported by the Directorate of Research and Community Service, Deputy for Strengthening Research and Development, Ministry of Research and Technology/National Research and Innovation Agency, Number: 150A/WM01.5/N/2021.

References

Abdelhameed, R.M., Abdel-Gawad, H., Elshahat, M., Emam, H.E., 2016. Cu–BTC@ cotton composite: design and removal of ethion insecticide from water. RSC Adv. 6 (48), 42324–42333.

Abdelhameed, R.M., Abdel-Gawad, H., Emam, H.E., 2021a. Macroporous Cu-MOF@ cellulose acetate membrane serviceable in selective removal of dimethoate pesticide from wastewater. J. Environ. Chem. Eng. 9 (2), 105121. https://doi.org/10.1016/j.jece:2021.105121.

Abdelhameed, R.M., Taha, M., Abdel-Gawad, H., Hegazi, B., 2021b. Amino-functionalized Al-MIL-53 for dimethoate pesticide removal from wastewater and their intermolecular interactions. J. Mol. Liq. 327, 114852. https://doi.org/10.1016/j.molliq.2020.114852.

Abdelhameed, R.M., Taha, M., Abdel-Gawad, H., Mahdy, F., Hegazi, B., 2019. Zeolitic imidazolate frameworks: Experimental and molecular simulation studies for efficient capture of pesticides from wastewater. J. Environ. Chem. Eng. 7 (6), 103499. https://doi.org/10.1016/j.jece:2019.103499.

Ahmed, I., Panja, T., Khan, N.A., Sarker, M., Yu, J.-S., Jhung, S.H., 2017. Nitrogen-doped porous carbons from ionic liquids@ MOF: remarkable adsorbents for both aqueous and nonaqueous media. ACS Appl. Mater. Interfaces 9 (11), 10276–10285.

Akpinar, I., Drout, R.J., Islamoglu, T., Kato, S., Lyu, J., Farha, O.K., 2019. Exploiting π–π interactions to design an efficient sorbent for atrazine removal from water. ACS Appl. Mater. Interfaces 11 (6), 6097–6103.

Akpinar, I., Yazaydin, A.O., 2018. Adsorption of atrazine from water in metal–organic framework materials. J. Chem. Eng. Data 63 (7), 2368–2375.

Al-Ghouti, M.A., Da'ana, D.A., 2020. Guidelines for the use and interpretation of adsorption isotherm models: A review. J. Hazard. Mater. 393, 122383. https://doi.org/10.1016/j.jhazmat.2020.122383.

Ali, I., Alharbi, O.M.L., ALOthman, Z.A., Al-Mohaimeed, A.M., Alwarthan, A., 2019. Modeling of fenuron pesticide adsorption on CNTs for mechanistic insight and removal in water. Environ. Res. 170, 389–397.

Anastopoulos, I., Kyzas, G.Z., 2016. Are the thermodynamic parameters correctly estimated in liquid-phase adsorption phenomena? J. Mol. Liq. 218, 174–185.

Ayawei, N., Ebelegi, A.N., Wankasi, D., 2017. Modelling and Interpretation of Adsorption Isotherms. J. Chem. 2017, 1–11.

Bansal, R.C., Goyal, M., 2005. Activated carbon adsorption. CRC Press.

Baumann, A.E., Burns, D.A., Liu, B., Thoi, V.S., 2019. Metal-organic framework functionalization and design strategies for advanced electrochemical energy storage devices. Commun. Chem. 2, 1–14.

Bhadra, B.N., Yoo, D.K., Jhung, S.H., 2020. Carbon-derived from metal-organic framework MOF-74: A remarkable adsorbent to remove a wide range of contaminants of emerging concern from water. Appl. Surf. Sci. 504, 144348. https://doi.org/10.1016/j.apsusc.2019.144348.

Bosch, M., Yuan, S., Rutledge, W., Zhou, H.-C., 2017. Stepwise synthesis of metal–organic frameworks. Acc. Chem. Res. 50 (4), 857–865.

Burtch, N.C., Jasuja, H., Walton, K.S., 2014. Water stability and adsorption in metal–organic frameworks. Chem. Rev. 114 (20), 10575–10612.

Cavka, J.H., Jakobsen, S., Olsbye, U., Guillou, N., Lamberti, C., Bordiga, S., Lillerud, K.P., 2008. A new zirconium inorganic building brick forming metal organic frameworks with exceptional stability. J. Am. Chem. Soc. 130 (42), 13850–13851.

Chapman, K.W., Halder, G.J., Chupas, P.J., 2009. Pressure-induced amorphization and porosity modification in a metal− organic framework. J. Am. Chem. Soc. 131 (48), 17546–17547.

Chen, B., Yang, Z., Zhu, Y., Xia, Y., 2014. Zeolitic imidazolate framework materials: recent progress in synthesis and applications. J. Mater. Chem. A 2 (40), 16811–16831.

Chen, D., Chen, C., Shen, W., Quan, H., Chen, S., Xie, S., Luo, X., Guo, L., 2017. MOF-derived magnetic porous carbon-based sorbent: synthesis, characterization, and adsorption behavior of organic micropollutants. Adv. Powder Technol. 28 (7), 1769–1779.

Chen, Y.-Z., Zhang, R., Jiao, L., Jiang, H.-L., 2018. Metal–organic framework-derived porous materials for catalysis. Coord. Chem. Rev. 362, 1–23.

Clark, C.A., Heck, K.N., Powell, C.D., Wong, M.S., 2019. Highly defective UiO-66 materials for the adsorptive removal of perfluorooctanesulfonate. ACS Sustainable Chem. Eng. 7 (7), 6619–6628.

Cosgrove, S., Jefferson, B., Jarvis, P., 2019. Pesticide removal from drinking water sources by adsorption: a review. Environ. Technol. Rev. 8 (1), 1–24.

Coudert, F.-X., Fuchs, A.H., 2016. Computational characterization and prediction of metal–organic framework properties. Coord. Chem. Rev. 307, 211–236.

De Smedt, C., Spanoghe, P., Biswas, S., Leus, K., Van Der Voort, P., 2015. Comparison of different solid adsorbents for the removal of mobile pesticides from aqueous solutions. Adsorption 21 (3), 243–254.

Devic, T., Serre, C., 2014. High valence 3p and transition metal based MOFs. Chem. Soc. Rev. 43 (16), 6097–6115.

Ding, M., Cai, X., Jiang, H.-L., 2019. Improving MOF stability: approaches and applications. Chem. Sci. 10 (44), 10209–10230.

Abdelillah Ali Elhussein, E., Şahin, S., Bayazit, Ş.S., 2018. Preparation of CeO2 nanofibers derived from Ce-BTC metal-organic frameworks and its application on pesticide adsorption. J. Mol. Liq. 255, 10–17.

Fang, Z., Bueken, B., DeVos, D.E., Fischer, R.A., 2015. Defect-engineered metal–organic frameworks. Angew. Chem. Int. Ed. 54 (25), 7234–7254.

Feng, D., Gu, Z.-Y., Li, J.-R., Jiang, H.-L., Wei, Z., Zhou, H.-C., 2012. Zirconium-metalloporphyrin PCN-222: mesoporous metal–organic frameworks with ultrahigh stability as biomimetic catalysts. Angew. Chem. Int. Ed. 51 (41), 10307–10310.

Feng, D., Xia, Y., 2018. Comparisons of glyphosate adsorption properties of different functional Cr-based metal–organic frameworks. J. Sep. Sci. 41 (3), 732–739.

Férey, G., Latroche, M., Serre, C., Millange, F., Loiseau, T., Percheron-Guégan, A., 2003. Hydrogen adsorption in the nanoporous metal-benzenedicarboxylate M (OH)(O 2 C-C 6 H 4–CO 2)(M= Al 3+, Cr 3+), MIL-53. Chem. Commun. (24), 2976–2977. https://doi.org/10.1039/B308903G.

Férey, G., Mellot-Draznieks, C., Serre, C., Millange, F., Dutour, J., Surblé, S., Margiolaki, I., 2005. A chromium terephthalate-based solid with unusually large pore volumes and surface area. Science 309 (5743), 2040–2042.

Foo, K.Y., Hameed, B.H., 2010. Insights into the modeling of adsorption isotherm systems. Chem. Eng. J. 156 (1), 2–10.

Guan, H.-Y., LeBlanc, R.J., Xie, S.-Y., Yue, Y., 2018. Recent progress in the syntheses of mesoporous metal–organic framework materials. Coord. Chem. Rev. 369, 76–90.

Hasan, Z., Choi, E.-J., Jhung, S.H., 2013. Adsorption of naproxen and clofibric acid over a metal–organic framework MIL-101 functionalized with acidic and basic groups. Chem. Eng. J. 219, 537–544.

Hinterholzinger, F., Scherb, C., Ahnfeldt, T., Stock, N., Bein, T., 2010. Oriented growth of the functionalized metal–organic framework CAU-1 on–OH-and–COOH-terminated self-assembled monolayers. PCCP 12 (17), 4515. https://doi.org/10.1039/b924657f.

Horcajada, P., Chalati, T., Serre, C., Gillet, B., Sebrie, C., Baati, T., Eubank, J.F., Heurtaux, D., Clayette, P., Kreuz, C., 2010. Porous metal–organic-framework nanoscale carriers as a potential platform for drug delivery and imaging. Nat. Mater. 9, 172–178.

Howarth, A.J., Liu, Y., Li, P., Li, Z., Wang, T.C., Hupp, J.T., Farha, O.K., 2016. Chemical, thermal and mechanical stabilities of metal–organic frameworks. Nat. Rev. Mater. 1, 1–15.

Huang, X., Feng, S., Zhu, G., Zheng, W., Shao, C., Zhou, N., Meng, Q.i., 2020. Removal of organic herbicides from aqueous solution by ionic liquid modified chitosan/metal-organic framework composite. Int. J. Biol. Macromol. 149, 882–892.

Jamali, A., Shemirani, F., Morsali, A., 2019. A comparative study of adsorption and removal of organophosphorus insecticides from aqueous solution by Zr-based MOFs. J. Ind. Eng. Chem. 80, 83–92.

Jiang, H.-L., Makal, T.A., Zhou, H.-C., 2013. Interpenetration control in metal–organic frameworks for functional applications. Coord. Chem. Rev. 257 (15-16), 2232–2249.

Jin, E., Lee, S., Kang, E., Kim, Y., Choe, W., 2020. Metal-organic frameworks as advanced adsorbents for pharmaceutical and personal care products. Coord. Chem. Rev. 425, 213526. https://doi.org/10.1016/j.ccr.2020.213526.

Joseph, L., Jun, B.-M., Jang, M., Park, C.M., Muñoz-Senmache, J.C., Hernández-Maldonado, A.J., Heyden, A., Yu, M., Yoon, Y., 2019. Removal of contaminants of emerging concern by metal-organic framework nanoadsorbents: A review. Chem. Eng. J. 369, 928–946.

Jung, B.K., Hasan, Z., Jhung, S.H., 2013. Adsorptive removal of 2, 4-dichlorophenoxy-acetic acid (2, 4-D) from water with a metal–organic framework. Chem. Eng. J. 234, 99–105.

Kandiah, M., Nilsen, M.H., Usseglio, S., Jakobsen, S., Olsbye, U., Tilset, M., Larabi, C., Quadrelli, E.A., Bonino, F., Lillerud, K.P., 2010. Synthesis and stability of tagged UiO-66 Zr-MOFs. Chem. Mater. 22 (24), 6632–6640.

Keskin, S., Kızılel, S., 2011. Biomedical applications of metal organic frameworks. Ind. Eng. Chem. Res. 50 (4), 1799–1812.

Kim, K.-H., Kabir, E., Jahan, S.A., 2017. Exposure to pesticides and the associated human health effects. Sci. Total Environ. 575, 525–535.

Kim, M.L., Otal, E.H., Hinestroza, J.P., 2019. Cellulose meets reticular chemistry: interactions between cellulosic substrates and metal–organic frameworks. Cellulose 26 (1), 123–137.

Kumar, S., Jain, S., Nehra, M., Dilbaghi, N., Marrazza, G., Kim, K.-H., 2020. Green synthesis of metal–organic frameworks: A state-of-the-art review of potential environmental and medical applications. Coord. Chem. Rev. 420, 213407. https://doi.org/10.1016/j.ccr.2020.213407.

Lee, JeongYong, Farha, O.K., Roberts, J., Scheidt, K.A., Nguyen, S.T., Hupp, J.T., 2009. Metal–organic framework materials as catalysts. Chem. Soc. Rev. 38 (5), 1450. https://doi.org/10.1039/b807080f.

Lei, C., Zhu, X., Zhu, B., Jiang, C., Le, Y., Yu, J., 2017. Superb adsorption capacity of hierarchical calcined Ni/Mg/Al layered double hydroxides for Congo red and Cr (VI) ions. J. Hazard. Mater. 321, 801–811.

Lei, J., Qian, R., Ling, P., Cui, L., Ju, H., 2014. Design and sensing applications of metal–organic framework composites. TrAC, Trends Anal. Chem. 58, 71–78.

Li, B., Wen, H.-M., Cui, Y., Zhou, W., Qian, G., Chen, B., 2016a. Emerging multifunctional metal–organic framework materials. Adv. Mater. 28 (40), 8819–8860.

Li, H., Shi, W., Zhao, K., Li, H., Bing, Y., Cheng, P., 2012. Enhanced hydrostability in Ni-doped MOF-5. Inorg. Chem. 51 (17), 9200–9207.

Li, J., Wang, X., Zhao, G., Chen, C., Chai, Z., Alsaedi, A., Hayat, T., Wang, X., 2018. Metal–organic framework-based materials: superior adsorbents for the capture of toxic and radioactive metal ions. Chem. Soc. Rev. 47 (7), 2322–2356.

Li, S., Feng, F., Chen, S., Zhang, X., Liang, Y., Shan, S., 2020a. Preparation of UiO-66-NH2 and UiO-66-NH2/sponge for adsorption of 2, 4-dichlorophenoxyacetic acid in water. Ecotoxicol. Environ. Saf. 194, 110440. https://doi.org/10.1016/j.ecoenv.2020.110440.

Li, T., Lu, M., Gao, Y., Huang, X., Liu, G., Xu, D., 2020b. Double layer MOFs M-ZIF-8@ZIF-67: The adsorption capacity and removal mechanism of fipronil and its metabolites from environmental water and cucumber samples. J. Adv. Res. 24, 159–166.

Li, W.-J., Tu, M., Cao, R., Fischer, R.A., 2016b. Metal–organic framework thin films: electrochemical fabrication techniques and corresponding applications & perspectives. J. Mater. Chem. A 4, 12356–12369.

Li, X., Zhang, L.i., Yang, Z., Wang, P., Yan, Y., Ran, J., 2020c. Adsorption materials for volatile organic compounds (VOCs) and the key factors for VOCs adsorption process: A review. Sep. Purif. Technol. 235, 116213. https://doi.org/10.1016/j.seppur.2019.116213.

Liang, W., Wang, B., Cheng, J., Xiao, D., Xie, Z., Zhao, J., 2021. 3D, eco-friendly metal-organic frameworks@ carbon nanotube aerogels composite materials for removal of pesticides in water. J. Hazard. Mater. 401, 123718. https://doi.org/10.1016/j.jhazmat.2020.123718.

Lima, E.C., Hosseini-Bandegharaei, A., Moreno-Piraján, J.C., Anastopoulos, I., 2019. A critical review of the estimation of the thermodynamic parameters on adsorption equilibria. Wrong use of equilibrium constant in the Van't Hoof equation for calculation of thermodynamic parameters of adsorption. J. Mol. Liq. 273, 425–434.

Liu, C., Wang, P., Liu, X., Yi, X., Zhou, Z., Liu, D., 2019a. Multifunctional β-cyclodextrin MOF-derived porous carbon as efficient herbicides adsorbent and potassium fertilizer. ACS Sustainable Chem. Eng. 7 (17), 14479–14489.

Liu, G., Li, L., Huang, X., Zheng, S., Xu, X., Liu, Z., Zhang, Y., Wang, J., Lin, H., Xu, D., 2018. Adsorption and removal of organophosphorus pesticides from environmental water and soil samples by using magnetic multi-walled carbon nanotubes@ organic framework ZIF-8. J. Mater. Sci. 53 (15), 10772–10783.

Liu, G., Li, L., Xu, D., Huang, X., Xu, X., Zheng, S., Zhang, Y., Lin, H., 2017. Metal–organic framework preparation using magnetic graphene oxide–β-cyclodextrin for neonicotinoid pesticide adsorption and removal. Carbohydr. Polym. 175, 584–591.

Liu, T., Xu, S., Lu, S., Qin, P., Bi, B., Ding, H., Liu, Y., Guo, X., Liu, X., 2019b. A review on removal of organophosphorus pesticides in constructed wetland: performance, mechanism and influencing factors. Sci. Total Environ. 651, 2247–2268.

Long, J.R., Yaghi, O.M., 2009. The pervasive chemistry of metal–organic frameworks. Chem. Soc. Rev. 38 (5), 1213. https://doi.org/10.1039/b903811f.

Lu, Z.-H., Abdelhai Senosy, I., Zhou, D.-D., Yang, Z.-H., Guo, H.-M., Liu, X., 2021. Synthesis and adsorption properties investigation of Fe3O4@ZnAl-LDH@MIL-53(Al) for azole fungicides removal from environmental water. Sep. Purif. Technol. 276, 119282. https://doi.org/10.1016/j.seppur.2021.119282.

Lv, X.-L., Yuan, S., Xie, L.-H., Darke, H.F., Chen, Y.a., He, T., Dong, C., Wang, B., Zhang, Y.-Z., Li, J.-R., Zhou, H.-C., 2019. Ligand rigidification for enhancing the stability of metal–organic frameworks. J. Am. Chem. Soc. 141 (26), 10283–10293.

Lyu, J., Zhang, N., Liu, H., Zeng, Z., Zhang, J., Bai, P., Guo, X., 2017. Adsorptive removal of boron by zeolitic imidazolate framework: kinetics, isotherms, thermodynamics, mechanism and recycling. Sep. Purif. Technol. 187, 67–75.

Ma, S., Sun, D., Simmons, J.M., Collier, C.D., Yuan, D., Zhou, H.-C., 2008. Metal-organic framework from an anthracene derivative containing nanoscopic cages exhibiting high methane uptake. J. Am. Chem. Soc. 130 (3), 1012–1016.

Mirsoleimani-azizi, S.M., Setoodeh, P., Samimi, F., Shadmehr, J., Hamedi, N., Rahimpour, M.R., 2018. Diazinon removal from aqueous media by mesoporous MIL-101 (Cr) in a continuous fixed-bed system. J. Environ. Chem. Eng. 6 (4), 4653–4664.

Mojiri, A., Zhou, J.L., Robinson, B., Ohashi, A., Ozaki, N., Kindaichi, T., Farraji, H., Vakili, M., 2020. Pesticides in aquatic environments and their removal by adsorption methods. Chemosphere 253, 126646. https://doi.org/10.1016/j.chemosphere.2020.126646.

Mouchaham, G., Wang, S., Serre, C., 2018. The stability of metal–organic frameworks. In: García, H., Navalón, S. (Eds.), Metal-Organic Frameworks: Applications in Separations and Catalysis. Wiley-VCH Verlag GmbH & Co. KGaA, Weinheim, Germany, pp. 1–28. https://doi.org/10.1002/9783527809097.ch1.

Moumen, E., Assen, A.H., Adil, K., Belmabkhout, Y., 2021. Versatility vs stability. Are the assets of metal–organic frameworks deployable in aqueous acidic and basic media? Coord. Chem. Rev. 443, 214020. https://doi.org/10.1016/j.ccr.2021.214020.

Nadar, S.S., Vaidya, L., Maurya, S., Rathod, V.K., 2019. Polysaccharide based metal organic frameworks (polysaccharide–MOF): A review. Coord. Chem. Rev. 396, 1–21.

Sheikhi, Z.N., Khajeh, M., Oveisi, A.R., Bohlooli, M., 2021. Functionalization of an iron-porphyrinic metal-organic framework with Bovine serum albumin for effective removal of organophosphate insecticides. J. Mol. Liq. 343, 116974. https://doi.org/10.1016/j.molliq.2021.116974.

Øien-Ødegaard, S., Bouchevreau, B., Hylland, K., Wu, L., Blom, R., Grande, C., Olsbye, U., Tilset, M., Lillerud, K.P., 2016. UiO-67-type metal–organic frameworks with enhanced water stability and methane adsorption capacity. Inorg. Chem. 55 (5), 1986–1991.

Pankajakshan, A., Sinha, M., Ojha, A.A., Mandal, S., 2018. Water-stable nanoscale zirconium-based metal–organic frameworks for the effective removal of glyphosate from aqueous media. ACS Omega 3 (7), 7832–7839.

Patil, D.V., Rallapalli, P.B.S., Dangi, G.P., Tayade, R.J., Somani, R.S., Bajaj, H.C., 2011. MIL-53 (Al): an efficient adsorbent for the removal of nitrobenzene from aqueous solutions. Ind. Eng. Chem. Res. 50 (18), 10516–10524.

Plazinski, W., Rudzinski, W., Plazinska, A., 2009. Theoretical models of sorption kinetics including a surface reaction mechanism: a review. Adv. Colloid Interface Sci. 152 (1-2), 2–13.

Qiu, H., Lv, L.u., Pan, B.-C., Zhang, Q.-J., Zhang, W.-M., Zhang, Q.-X., 2009. Critical review in adsorption kinetic models. J. Zhejiang Univ.-Sci. A 10 (5), 716–724.

Redfern, L.R., Farha, O.K., 2019. Mechanical properties of metal–organic frameworks. Chem. Sci. 10 (46), 10666–10679.

Ren, J., Ledwaba, M., Musyoka, N.M., Langmi, H.W., Mathe, M., Liao, S., Pang, W., 2017. Structural defects in metal–organic frameworks (MOFs): Formation, detection and control towards practices of interests. Coord. Chem. Rev. 349, 169–197.

Sabarwal, A., Kumar, K., Singh, R.P., 2018. Hazardous effects of chemical pesticides on human health–Cancer and other associated disorders. Environ. Toxicol. Pharmacol. 63, 103–114.

Safaei, M., Foroughi, M.M., Ebrahimpoor, N., Jahani, S., Omidi, A., Khatami, M., 2019. A review on metal-organic frameworks: Synthesis and applications. TrAC, Trends Anal. Chem. 118, 401–425.

Saha, P., Chowdhury, S., 2011. In: Thermodynamics. InTech. https://doi.org/10.5772/13474.

Saleh, I.A., Zouari, N., Al-Ghouti, M.A., 2020. Removal of pesticides from water and wastewater: Chemical, physical and biological treatment approaches. Environ. Technol. Innov. 19, 101026. https://doi.org/10.1016/j.eti.2020.101026.

Sarker, M., Ahmed, I., Jhung, S.H., 2017. Adsorptive removal of herbicides from water over nitrogen-doped carbon obtained from ionic liquid@ ZIF-8. Chem. Eng. J. 323, 203–211.

Sarker, M., Song, J.Y., Jhung, S.H., 2018. Carboxylic-acid-functionalized UiO-66-NH2: a promising adsorbent for both aqueous-and non-aqueous-phase adsorptions. Chem. Eng. J. 331, 124–131.

Seo, Y.S., Khan, N.A., Jhung, S.H., 2015. Adsorptive removal of methylchlorophenoxypropionic acid from water with a metal-organic framework. Chem. Eng. J. 270, 22–27.

Shimizu, G.K.H., Vaidhyanathan, R., Taylor, J.M., 2009. Phosphonate and sulfonate metal organic frameworks. Chem. Soc. Rev. 38 (5), 1430. https://doi.org/10.1039/b802423p.

Singh, S., Kaushal, S., Kaur, J., Kaur, G., Mittal, S.K., Singh, P.P., 2021. CaFu MOF as an efficient adsorbent for simultaneous removal of imidacloprid pesticide and cadmium ions from wastewater. Chemosphere 272, 129648. https://doi.org/10.1016/j.chemosphere.2021.129648.

Stock, N., Biswas, S., 2012. Synthesis of metal-organic frameworks (MOFs): routes to various MOF topologies, morphologies, and composites. Chem. Rev. 112 (2), 933–969.

Sun, X., Wu, T., Yan, Z., Chen, W.-J., Lian, X.-B., Xia, Q., Chen, S., Wu, Q.-H., 2019. Novel MOF-5 derived porous carbons as excellent adsorption materials for n-hexane. J. Solid State Chem. 271, 354–360.

Tan, K.L., Foo, K.Y., 2021. Preparation of MIL-100 via a novel water-based heatless synthesis technique for the effective remediation of phenoxyacetic acid-based pesticide. J. Environ. Chem. Eng. 9 (1), 104923. https://doi.org/10.1016/j.jece:2020.104923.

Taylor, J.M., Vaidhyanathan, R., Iremonger, S.S., Shimizu, G.K.H., 2012. Enhancing water stability of metal–organic frameworks via phosphonate monoester linkers. J. Am. Chem. Soc. 134 (35), 14338–14340.

Uddin, M.J., Ampiaw, R.E., Lee, W., 2021. Adsorptive removal of dyes from wastewater using a metal-organic framework: A review. Chemosphere 284, 131314. https://doi.org/10.1016/j.chemosphere.2021.131314.

Vogt, E.T.C., Weckhuysen, B.M., 2015. Fluid catalytic cracking: recent developments on the grand old lady of zeolite catalysis. Chem. Soc. Rev. 44 (20), 7342–7370.

Wang, C., Liu, X., Keser Demir, N., Chen, J.P., Li, K., 2016. Applications of water stable metal–organic frameworks. Chem. Soc. Rev. 45 (18), 5107–5134.

Wang, J., Guo, X., 2020. Adsorption isotherm models: Classification, physical meaning, application and solving method. Chemosphere 258, 127279. https://doi.org/10.1016/j.chemosphere.2020.127279.

Wu, G., Ma, J., Li, S., Wang, S., Jiang, B.o., Luo, S., Li, J., Wang, X., Guan, Y., Chen, L., 2020. Cationic metal-organic frameworks as an efficient adsorbent for the removal of 2, 4-dichlorophenoxyacetic acid from aqueous solutions. Environ. Res. 186, 109542. https://doi.org/10.1016/j.envres.2020.109542.

Xiao, Y., Chen, C., Wu, Y., Wang, J., Yin, Y., Chen, J., Huang, X., Qi, P., Zheng, B., 2021. Water-stable Al-TCPP MOF nanosheets with hierarchical porous structure for removal of chlorantraniliprole in water. Micropor. Mesopor. Mater. 324, 111272. https://doi.org/10.1016/j.micromeso.2021.111272.

Xie, L., Liu, D., Huang, H., Yang, Q., Zhong, C., 2014. Efficient capture of nitrobenzene from waste water using metal–organic frameworks. Chem. Eng. J. 246, 142–149.

Xie, Y.i., Chen, C., Lu, X., Luo, F., Wang, C., Alsaedi, A., Hayat, T., 2019. Porous NiFe-oxide nanocubes derived from prussian blue analogue as efficient adsorbents for the removal of toxic metal ions and organic dyes. J. Hazard. Mater. 379, 120786. https://doi.org/10.1016/j.jhazmat.2019.120786.

Yang, C., Wang, X., Omary, M.A., 2007. Fluorous metal– organic frameworks for high-density gas adsorption. J. Am. Chem. Soc. 129 (50), 15454–15455.

Yang, J., Grzech, A., Mulder, F.M., Dingemans, T.J., 2011. Methyl modified MOF-5: a water stable hydrogen storage material. Chem. Commun. 47 (18), 5244. https://doi.org/10.1039/c1cc11054c.

Yang, L.-M., Ganz, E., Svelle, S., Tilset, M., 2014. Computational exploration of newly synthesized zirconium metal–organic frameworks UiO-66,-67,-68 and analogues. J. Mater. Chem. C 2 (34), 7111–7125.

Yang, Q., Wang, J., Chen, X., Yang, W., Pei, H., Hu, N.a., Li, Z., Suo, Y., Li, T., Wang, J., 2018. The simultaneous detection and removal of organophosphorus pesticides by a novel Zr-MOF based smart adsorbent. J. Mater. Chem. A 6 (5), 2184–2192.

Yang, Q., Wang, J., Zhang, W., Liu, F., Yue, X., Liu, Y., Yang, M., Li, Z., Wang, J., 2017. Interface engineering of metal organic framework on graphene oxide with enhanced adsorption capacity for organophosphorus pesticide. Chem. Eng. J. 313, 19–26.

Yang, Y., Che, J., Wang, B., Wu, Y., Chen, B., Gao, L., Dong, X., Zhao, J., 2019. Visible-light-mediated guest trapping in a photosensitizing porous coordination network: metal-free C-C bond-forming modification of metal–organic frameworks for aqueous-phase herbicide adsorption. Chem. Commun. 55 (37), 5383–5386.

Yao, Q., Bermejo Gómez, A., Su, J., Pascanu, V., Yun, Y., Zheng, H., Chen, H., Liu, L., Abdelhamid, H.N., Martín-Matute, B., Zou, X., 2015. Series of highly stable isoreticular lanthanide metal–organic frameworks with expanding pore size and tunable luminescent properties. Chem. Mater. 27 (15), 5332–5339.

Yin, Z., Wan, S., Yang, J., Kurmoo, M., Zeng, M.-H., 2019. Recent advances in post-synthetic modification of metal–organic frameworks: New types and tandem reactions. Coord. Chem. Rev. 378, 500–512.

Yu, F., Bai, X., Liang, M., Ma, J., 2021. Recent progress on metal-organic framework-derived porous carbon and its composite for pollutant adsorption from liquid phase. Chem. Eng. J. 405, 126960. https://doi.org/10.1016/j.cej.2020.126960.

Yuan, S., Feng, L., Wang, K., Pang, J., Bosch, M., Lollar, C., Sun, Y., Qin, J., Yang, X., Zhang, P., Wang, Q.i., Zou, L., Zhang, Y., Zhang, L., Fang, Y.u., Li, J., Zhou, H.-C., 2018. Stable metal–organic frameworks: design, synthesis, and applications. Adv. Mater. 30 (37), 1704303. https://doi.org/10.1002/adma.v30.3710.1002/adma.201704303.

Zhang, J., Cai, Y., Liu, K., 2019a. Extremely effective boron removal from water by stable metal organic framework ZIF-67. Ind. Eng. Chem. Res. 58 (10), 4199–4207.

Zhang, W., Hu, Y., Ge, J., Jiang, H.-L., Yu, S.-H., 2014. A facile and general coating approach to moisture/water-resistant metal–organic frameworks with intact porosity. J. Am. Chem. Soc. 136 (49), 16978–16981.

Zhang, Y., Zhu, C., Liu, F., Yuan, Y., Wu, H., Li, A., 2019b. Effects of ionic strength on removal of toxic pollutants from aqueous media with multifarious adsorbents: A review. Sci. Total Environ. 646, 265–279.

Zhu, Q.-L., Xu, Q., 2014. Metal–organic framework composites. Chem. Soc. Rev. 43 (16), 5468–5512.

Zhu, X., Li, B., Yang, J., Li, Y., Zhao, W., Shi, J., Gu, J., 2015. Effective adsorption and enhanced removal of organophosphorus pesticides from aqueous solution by Zr-based MOFs of UiO-67. ACS Appl. Mater. Interfaces 7 (1), 223–231.

Zu, D.-D., Lu, L., Liu, X.-Q., Zhang, D.-Y., Sun, L.-B., 2014. Improving hydrothermal stability and catalytic activity of metal–organic frameworks by graphite oxide incorporation. J. Phys. Chem. C 118 (34), 19910–19917.